University of Southern Queensland

Faculty of Health, Engineering and Sciences

SENSOR TO IMPROVE DETECTION OF LINE BREAK OR EARTH FAULTS FOR VICTORIAN SWER LINES

A dissertation submitted by

Benjamin Stephens

In fulfilment of the requirements of

ENG4111 & ENG4112 Research Project

Towards the degree of

Bachelor of Engineering (Honours)

(Electrical & Electronic)

Submitted October 2016

Abstract

This project is an investigation into a possible fault detection system for SWER (single wire earth return) electrical distribution networks in Victoria that focuses on types of faults that are undetectable by conventional protection systems and have the ability to ignite fires. The paper considers why a new detection system is required and then how it could be practically implemented in a general sense. More detailed investigations then focus on communications, power harvesting and fault detection considerations.

The devices are proposed to be distributed across SWER networks to enact a detection system. The paper focuses on the many conflicting requirements and subsequent compromises that any eventual design will need to overcome. It is found that electric field power harvesting from the Victorian SWER lines' 12.7kV conductor can produce power outputs within the range required by standalone detection devices given fairly severe design constraints. Summaries and conclusions are drawn to a level where the project develops a clear methodology to go forward.

University of Southern Queensland

Faculty of Health, Engineering and Sciences

ENG4111 & ENG4112 Research Project

Limitations of Use

The Council of the University of Southern Queensland, its Faculty of Health, Engineering and Science, and the staff of the University of Southern Queensland, do not accept any responsibility for the truth, accuracy or completeness of material contained within or associated with this dissertation.

Persons using all or any part of this material do so at their own risk, and not at the risk of the Council of the University of Southern Queensland, its Faculty of Health, Engineering and Sciences, or the staff of the University of Southern Queensland.

This dissertation reports an educational exercise and has no purpose or validity beyond this exercise. The sole purpose of the course pair entitles 'Research Project' is to contribute to the overall education within the student's chosen degree program. This document, the associated hardware, software, drawings, and any other material set out in the associated appendices should not be used for any other purpose; if they are so used, it is entirely at the risk of the user.

Certification

I certify that the ideas, designs and experimental work, results, analyse conclusions set out in this dissertation are entirely my own effort, except otherwise indicated and acknowledged.

I further certify that the work is original and has not been previously submit assessment in any other course or institution, except where specifically stated

Benjamin Stephens

Student Number: 0061052083

Acknowledgements

Thanks are due to Andreas Helwig for supervision, guidance and inspiration and Catherine Hills for supervision and ‘special comments’ throughout the project.

To my Dad for his major assistance with the experiment set up and providing an adequate table tennis opponent during study breaks.

To my Mum for allowing us to experiment with 240V equipment, but more importantly being a never ending source of support and encouragement.

To Jarden for providing the first line of defence against the real world whilst studies were in progress and bankrolling the project and the broader bachelor degree even when purse strings were very tight – I can’t promise it was a good investment.

To Jamie for dragging me into all this University mess and helping me see it through.

To Coach for the constant reminder that sitting at the computer all day displeases him.

And to my immediate family as a whole, who have supported me through ongoing illness and some very dark times. I know I have been grumpy and sometimes insufferable but you put up with it and rarely let me know how much of a pain I was being. I intend on repaying the favour one day.

Thanks all,

Ben

Contents

Abstract ... iii

Certification ... v

Acknowledgements ... vi

List of Figures ... xii

List of Tables ... xiv

1 Introduction ... 1

1.1 Electricity Caused Bushfires ... 1

1.2 Project Aims ... 2

1.3 Justification: The Victorian Bushfire Royal Commission ... 2

1.3.1 Single Wire Earth Return (SWER) protection problems ... 3

1.3.2 Costs of SWER upgrades ... 3

1.3.3 New approaches to SWER protection and control ... 4

1.3.4 A Network of Detection Devices ... 5

1.3.5 Victoria SWER line networks ... 5

1.3.6 Quoted SWER Characteristics ... 6

2 Literature Reviews ... 7

2.1 Energy Harvesting ... 7

2.1.1 Introduction and Scope ... 7

2.1.2 Magnetic Induction ... 7

2.1.3 Electric Field ... 10

2.1.4 Piezoelectric ... 17

2.2 Communications ... 17

2.2.1 Introduction and Scope ... 17

2.2.2 Device Deployment locations and range limitation ... 18

2.2.3 Base Station/Gateway Deployment Locations ... 19

2.2.4 Data Traffic Requirements ... 19

2.2.5 Reliability ... 19

2.2.6 Wireless sensor networks ... 21

2.2.7 Physical Layer 22
2.2.8 Data – Link Layer 25
2.2.9 Network Layer 27
2.2.10 Transport and Application Layers 27
2.2.11 Mesh Networks 28
2.2.12 Hybrid Topologies 29
2.2.13 Wireless Mesh Networks 29
2.2.14 Range and radio propagation 31
2.2.15 Long Range Wireless Sensor Networks 33
2.2.16 Security 33
2.2.17 Power line communications (PLC) 34
2.3 Fault Detection 34
2.3.1 Existing Fault Protection 34
2.3.2 High Impedance Earth Faults and Arcing 35
2.3.3 Network device mapping 37
2.4 Summary 37
3 Methodology for Energy Harvesting 39
3.1 Introduction and Scope 39
3.2 Electrostatic Energy Harvesting Experiment 40
3.2.1 Experiment Aims 40
3.2.2 Simulation Model 40
3.2.3 Simulation Scenarios and Results 43
3.2.4 Final Designs 46
3.2.5 Lab Experiment 47
4 Fault Detection and Mapping Development 55
4.1 Introduction 55
4.2 Fault Detection 55
4.2.1 Arc Detection 56
4.2.2 Logical Open-Conductor Approach 57

4.2.3 Nodal Analysis Approach 59
4.3 Mapping 61
4.4 Contribution to Device Power Consumption 62
4.4.1 Sensing and Peripheral Circuitry 62
4.4.2 Processing 63
4.4.3 GPS 64
4.5 Fault and Protection Systems Integration 64
5 Communications System Specification 66
5.1 Introduction 66
5.1.1 A Word on Security 66
5.1.2 Presentation of Simultaneous Requirements 67
5.2 Communications Specification Discussion 68
5.2.1 Hardware and Modulation 68
5.2.2 Medium Access Control 68
5.3 Power Consumption Calculation 72
6 Results and Discussion 74
6.1 Chapter Overview 74
6.2 Energy Harvesting Experiment Results 74
6.2.1 System Capacitance Anomalies 74
6.2.2 Energy Harvester with Transformer Results 77
6.2.3 Main 240V Experiment Results 78
6.2.4 Model Performance Discussion 81
6.2.5 Extrapolation to 12.7kV SWER 81
6.3 Power Budget 88
6.4 Costing Estimates 89
7 Conclusions 90
7.1 Chapter Overview 90
7.2 Achievement of Project Objectives 90
7.3 Shortcomings and Possible Improvements 91

7.4 Further Work 92
8 References 93
Appendices 100
Appendix A – Project Specification 100
Appendix B – Quoted SWER Characteristics 101
Appendix C – Project Phase Breakdown 104
Appendix D – Matlab Electrostatic Harvester Model 105
Appendix E – Simulation Input Parameters and Output Figures 108
Appendix F – 240V Experiment Output Results 117

List of Figures

Figure 1.1 – Victorian SWER example (Helwig 2015).....6

Figure 2.1 – Magnetic Induction equivalent tuned circuit using Brooks coil (Tashiro et al 2011).....8

Figure 2.2 – Cylindrical electrode enclosing conductor (Keutel et al 2012).....11

Figure 2.3 – Capacitive Divider (Keutel et al 2012).....11

Figure 2.4 – Capacitive System with load (Zhao et al 2012).....12

Figure 2.5 – Simulated Power Output for Electric Field Harvester with varying load impedance.....14

Figure 2.6 – Simulated Harvester Voltage for Electric Field harvesting with varying load impedance.....15

Figure 2.7 – Range and redundancy limit – two consecutive node failures in a straight line resulting in a broken partial mesh.....20

Figure 2.8 – Adaption of the OSI layer system for wireless sensors (Akyildiz et al 2002).....22

Figure 2.9 – Mesh Topology (Cecilio & Furtado 2014).....28

Figure 3.1 – Electrostatic energy harvester schematic (adaption of circuit design by Zangl 2009).....41

Figure 3.2 – Equivalent AC reactances encountered by the harvester.....41

Figure 3.3 – Thevenin equivalent DC resistances as seen by the storage capacitor.....42

Figure 3.4A – Normal simulation – Zangl parameters.....44

Figure 3.4B – Low cut-off voltage using maximum slope for charging only simulation – Zangl parameters.....44

Figure 3.5A – Normal simulation – Zhao parameters.....44

Figure 3.5B – Low cut-off voltage using maximum slope for charging only simulation – Zhao parameters.....44

Figure 3.6A – Normal simulation – 12.7kV SWER.....45

Figure 3.6B – Low cut-off voltage using maximum slope for charging only simulation – 12.7kV SWER.....45

Figure 3.7A – Normal simulation – 240V Mains.....45

Figure 3.7B – Low cut-off voltage using maximum slope for charging only simulation – 240V Mains.....45

Figure 3.8 – Initial Circuit – Step down transformer included (circuit adapted from Zangl 2009).....46

Figure 3.9 – Second Circuit – Step down transformer removed (circuit adapted from Zangl 2009).....46

Figure 3.10 – Electric field energy harvesting experiment apparatus.....48

Figure 3.11 – Electrical field energy harvesting experiment close-up including transformer.....48

Figure 3.12 – Electrical field energy harvesting experiment close-up of charging circuit.....48

Figure 3.13 – Transformer with high magnetising inductance used in initial charging circuit.....49

Figure 3.14 – Equivalent test circuits to determine system capacitances present.....50

Figure 3.15 – Output from 240V harvester circuit simulation with transformer (circuit adapted from Zangl 2009).....51

Figure 3.16 – Output from 240V harvester simulation with transformer omitted (circuit adapted from Zangl 2009).....53

Figure 4.1 – Depiction of conductor break & response from downstream devices.....57

Figure 4.2 – Depiction of nodal analysis implementation.....59

Figure 4.3 – Schneider Electric W Series Remote Control ACR & associated control cabinets (Schneider Electric 2012).....64

Figure 4.4 – Typical Recloser – Sectionaliser deployment (Electrical Engineering Community 2016).....64

Figure 5.1 – Multiple hops between nodes causing TDMA delays (Djukic 2011).....69

Figure 5.2 – Cluster of nodes and their respective ‘conflicts graph’ (Djukic 2011).....69

Figure 6.1 – Method of images to determine shunt capacitance for single wire system (Glover & Sarma 1994).....75

Figure 6.2 – Actual charging waveforms vs. simulated waveforms from 240V scenario experiment.....77

Figure 6.3 – Drop off of peak to peak source current feeding harvester circuit from 240V simulation from experimental parameters.....79

Figure 6.4 – 12.7kV SWER simulation #1.....82

Figure 6.5 – 12.7kV SWER simulation #1 average power output.....83

Figure 6.6 – 12.7kV SWER simulation #2.....84

Figure 6.7 – 12.7kV SWER simulation #2 average power output.....85

List of Tables

Table 1.1 – Relative Costs to Upgrade Victorian SWER Networks (Parsons Brinckerhoff 2009).....4

Table 2.1 – Assorted RF chips with their power consumption attributes (Sourced from respective company datasheets).....23

Table 2.2 – Mesh Protocols Examples.....30

Table 2.3 – Summary of Technologies Reviewed.....38

Table 3.1 – Simulated Power Outputs (parameters gleaned from Zangl 2009 & Zhao 2012 experiment & put through Stephens 2016 simulation model).....43

Table 5.1 – Presentation of Wireless Communications Simultaneous Requirements.....66

Table 6.1 – Initial experiments with step down transformer included, with & without Digital Multimeter (ZIN = 9.16Ohm).....77

Table 6.2 – Estimated device power consumption breakdown.....86

Table 6.3 – Cost breakdown estimates for total Victorian SWER networks.....87

Nomenclature and acronyms

ACR	Automatic Circuit Recloser
ADC	Analogue to Digital Converter
CDMA	Code Division Medium Access
CSMA/CA	Carrier Sense Multiple Access with Collision Avoidance
DMM	Digital Multi Meter
EIRP	Equivalent Isotropically Radiated Power
FDMA	Frequency Division Multiple Access
FSK	Frequency Shift Keying
HIF	High Impedance Fault
ISM	Industrial Scientific and Medical bands
MAC	Medium Access Control
OCR	Oil filled Circuit Recloser
OFDM	Orthogonal Frequency Division Multiplexing
OOK	On Off Keying
QoS	Quality of Service
RMS	Root Mean Squared
SCADA	System Control and Data Aquisition
SNR	Signal to Noise Ratio
SWER	Single Wire Earth Return
TDMA	Time Domain Medium Access
WMN	Wireless Mesh Network
WSN	Wireless Sensor Network

1 Introduction

1.1 Electricity Caused Bushfires

The majority of bushfires in the Australian landscape are an unavoidable natural phenomenon. Their ferocity and level of destruction is governed by the amount of fuel present and the prevailing weather conditions. Given the right circumstances, catastrophic scenarios can occur such as when long, out of control fire fronts pass over inhabited areas.

This scenario has eventuated on a number of occasions throughout Australia's history, with "Ash Wednesday", "Black Friday" and more recently, "Black Saturday" being added to Australian vernacular. On Black Saturday, 7th February 2009, 173 people were reported to have lost their lives (ABC 2009). 119 of those were lost to the Kilmore East fire, which was ignited from a power pole fault (RVB 2010). This fact supports the opinion that more should be done to prevent avoidable 'man made' fire ignitions; especially ones developing form public infrastructure where risks such as this should be properly mitigated.

The electrical infrastructure starting the Kilmore East fire was not of the 'SWER' type of distribution that is the focus of this project; however, the risk that SWER lines pose was demonstrated by the ignition of the Coleraine bushfire, also on Black Saturday (RVB 2010).

1.2 Project Aims

The main aim of the project is:

To investigate the possibility of developing a robust and low cost sensitive fault detection and communications device for the existing Victorian SWER (single wire earth return) line network.

Objectives that support the main aim are:

- *To design a simple, reliable energy harvesting system that provides power to all device functions.*
- *To specify a meshed communications system that can support all alarm and condition monitoring data traffic.*
- *To design a logical based fault detection system that compares nodes condition monitoring data to identify faults not detectable by conventional methods.*
- *To specify the system and the individual device to a level where evaluation may be undertaken.*

1.3 Justification: The Victorian Bushfire Royal Commission

The 2009 Victorian Bushfire Royal Commission was undertaken as a result of the fallout from the Black Saturday bushfires. The Commission's report, along with other related reports, has identified the particular problem of SWER powerlines with regards to their inability to de-energise under every fault scenario. The commission deemed this extra risk as unacceptable, and as such included in recommendation number 27 that all SWER lines be progressively replaced with other technologies that significantly reduce the bushfire risk.

1.3.1 Single Wire Earth Return (SWER) protection problems

Single Wire Earth Return (SWER) powerlines account for close to 32% - or 28,000km – of Victoria's distribution network, and are comprised of a single exposed conductor suspended over relatively long spans (Holland 2013). The SWER network is based mainly in rural and remote areas; a significant proportion of which is prone to bushfires.

An inherent problem with SWER powerlines is the inability to detect, and thus protect against, sensitive earth faults. The return path for the flow of electricity occurs through the earth instead of a dedicated earth conductor as is the case with conventional multiple conductor powerlines. As a result the earth current flow is difficult to monitor, and so the ability to distinguish between current flowing through a normal load and that of a fault situation becomes more difficult (RVB 2010). Evidence at the Royal Commission was given by Mr Kim Griffith (State Electricity Commission of Victoria and past CEO of Ergon Energy) (RVB 2010) that inferred that SWER was 90 percent less effective than conventional distribution systems at detecting HIFs (High Impedance Faults) due to the return path being through the ground.

Clearly if live conductors remain live after a fault such as a wire break or vegetation coming into contact with the conductor, then the possibility of fire ignition is significantly increased.

1.3.2 Costs of SWER upgrades

A Recommendation of the Commission was for all Victorian SWER lines to be removed and replaced with safer alternatives (RVB 2010). The financial cost of installing these alternatives is in the many billions of dollars (Table 1.1), with the safest of technologies – underground cables – being the most expensive (Parsons Brinckerhoff 2009).

Table 1.1 – Relative costs to upgrade Victorian SWER networks (adaption from report by Parsons Brinckerhoff 2009)

Option	Description	Cost per Km	Total (28,000 km)
SWER (concrete poles)	Replacing like for like. Included here reference purposes.	**$32,244**	**$902,832,000**
CCT	Covered Conductor (Insulated SWER)	**$70,448**	**$1,960,000,000**
ABC	Aerial Bundled Cable (Three Phase Insulated)	**$126,759**	**$3,549,252,000**
Underground	Three Phase direct buried into the ground	**$168,240**	**$4,710,720,000**

The Victorian Government has acknowledged these recommendations but has yet to commit to a blanket replacement of SWER lines, opting instead to target the most dangerous power lines and to introduce new protection strategies and technologies (Citipower 2012)

1.3.3 New approaches to SWER protection and control

A report generated by the 'National Workshop on rural electricity network options to reduce bushfire risk', held by The Nous Group (2010), presents some differing views to the Commission in identifying ways of mitigating the risk of fire ignitions from SWER networks. The workshop report proposed that the application of new technologies to existing rural distribution systems could effectively mitigate the need for blanket replacements. Specifically the ability to detect HIFs and to dynamically adjust protection characteristics to account for periods of increased fire risk was highlighted. These enhanced abilities were proposed to be realised from modern automatic circuit reclosers and other digital remote control systems that incorporated radio based communications. The opportunities were said to have been part of ongoing investigations by stakeholders already and it is the intention of this project to follow a similar line of thinking.

1.3.4 A Network of Detection Devices

Proposed is the deployment of a network of reliable, low cost, communicating, 'self powering' devices spanning entire SWER networks, with the ability to detect and report upon electrical faults that may occur anywhere on the network. The devices are 'self powered' in that the energy required by the device is harvested from the energised SWER conductor. The inter device communication scheme could employ 'meshing' techniques, which provide greater levels of reliability. Finally, the fault detection function could detect wire break faults and other types of high impedance faults through the use of logic, using real-time Voltage and Current data from the devices.

The information from the device network could be fed into gateways or base stations that interface with existing control networks or protection equipment, Holland (2013), noted that where automatic reclosers are positioned provide convenient locations for new remote control or SCADA type systems to reside. This was in reference to remote data collection and other systems but the premise that new systems attempting to interface with SWER networks would be located here is applicable.

1.3.5 Victoria SWER line networks

Below is an example of a Victorian SWER line topology (Figure 1.1); depicted is a network being fed by a 100kVA isolation transformer to the left of the page. The black dots are positions indicating that there is a fork in the branch/trunk, or a 240V customer transformer is connected, and are likely the positions of strainer type power poles (they are supporting a change in direction for the power line which is under considerable tension). Not depicted are the suspension type poles that are generally there to support conductor spans continuing in the same direction. Average span lengths for SWER are 205m, according to a Parsons Brinckerhoff (2009) report, and so we would expect to see in the range of 1-3 suspension power poles placed between the strainer poles (black dots) on this map.

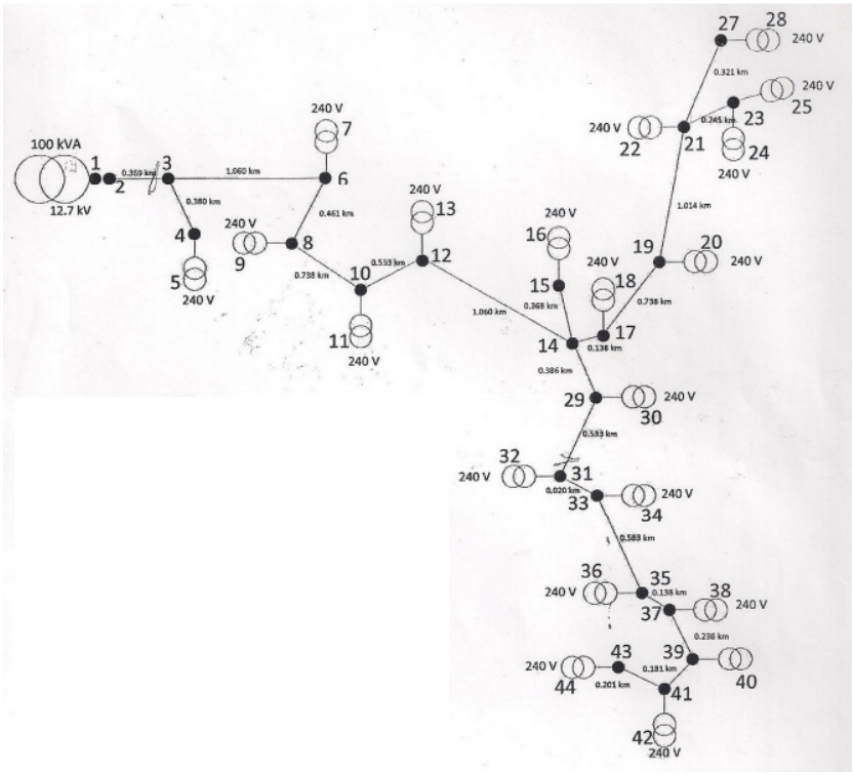

Figure 1.1 – Victorian SWER example (Helwig 2015)

1.3.6 Quoted SWER Characteristics

Appendix B – 'Quoted SWER Characteristics' contains relevant quoted values and figures for SWER line characteristics and their respective sources, used in this report.

2 Literature Reviews

2.1 Energy Harvesting

2.1.1 Introduction and Scope

A literature review was conducted to help find methods to best extract the energy from the electromagnetic field surrounding energised conductors. Methods more likely to achieve desired results or meet certain critical requirements were given more attention. The material presented reflects this mentality by following an 'investigative' approach rather than a more traditional 'survey of technologies' type approach.

The power requirements of the proposed device will be one of the most critical factors of the design; however the size, weight and shape of any energy harvesting apparatuses will also need to dominate a critical review of the available technologies.

Solar PV (photo voltaic) and wind harvesting technologies have not been considered for this project due to the variability of the energy sources and the burdensome mechanical requirements that would be placed upon the device.

To make judgements upon the suitability of various energy harvesting techniques, an initial investigation into the likely approximate minimum power levels was conducted.

The proposed device will likely have a number of functions that consume power. To obtain a 'ballpark' figure, this project focuses on the main areas expected to consume the vast majority of the power budget, such as communications and processing. For the purposes described, the required power budget is assumed to be a continuous 10mW.

2.1.2 Magnetic Induction

Magnetic induction harvesting techniques involve coupling the magnetic field that axially encircles the conductor when a current flows through it. A conductor within the changing magnetic field such as a 'Brooks coil', proposed by Tashiro et al (2011), will attempt to create its own field that opposes the change. An associated voltage will develop across

the coil terminals and a current is produced, assuming a load is placed across the terminals. The system can be thought of as a current transformer, where the primary winding is the conductor, and the secondary winding is the coil placed within the field.

The 50Hz AC current induced in the secondary can then be converted to DC via an AC to DC rectifier circuit, and then converted to the desired voltage using a DC to DC switching converter (Roscoe et al 2009). The output power produced is proportional to the amount of current flow in the conductor and is independent of the voltage level.

Tashiro et al (2011) proposes a 'Brooks coil' be used for the harvesting secondary coil due to the relative simplicity in obtaining specific inductance values, which are used to achieve resonance in what can be thought of as a tuned circuit; a capacitor is also added for this purpose. The equivalent series tuned circuit is shown in Figure 2.1.

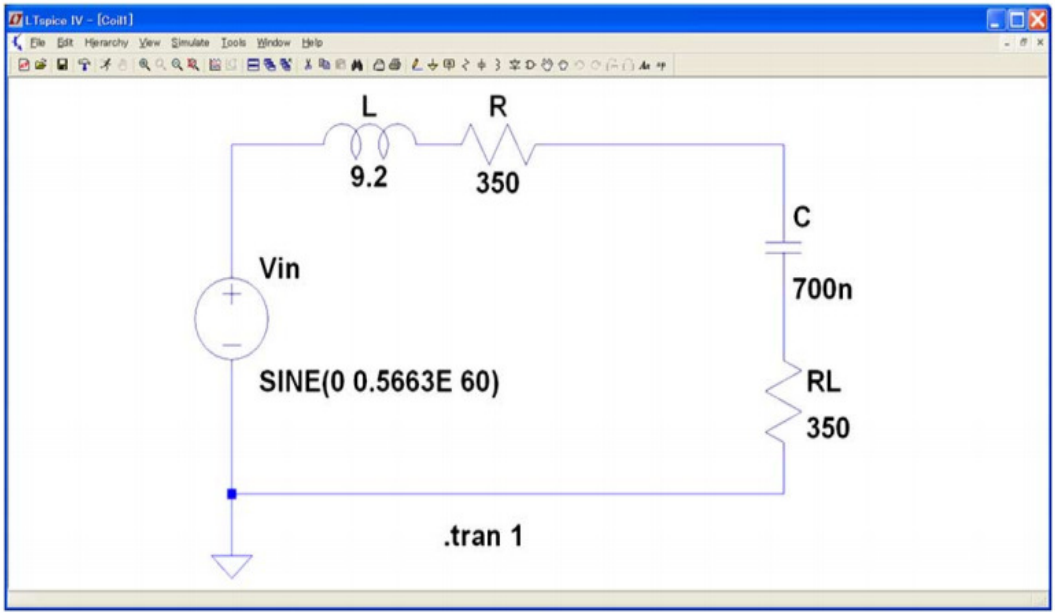

Figure 2.1 – Magnetic Induction equivalent tuned circuit using Brooks coil (Tashiro et al 2011)

It is explained by Tashiro et al (2011) that the induced voltage V_{in} can be calculated using a formula based on Faraday's law of induction and Thevenin's theorem (eqn 2.1).

$$V_{in} = 2\pi^2 fna^2 B \tag{2.1}$$

Where f (Hz) is the frequency, n and a^2 are the number of turns and the mean radius of the Brooks coil respectively, and B is the mean flux density orthogonal to the cross sectional area.

Power output can then be estimated using equation 2.2.

$$P = \frac{{V_{out}}^2}{R_L} \tag{2.2}$$

Where V_{Out} is the voltage across the load resistance R_L. For a given uniform magnetic field with flux density B = 21.2 $_{\mu}$T (micro Tesla), Tashiro et al (2010) was able to achieve 6.23mW of output power.

To relate and estimate the magnetic field's flux density to the current flowing through the wire we can use the formula that assumes an infinitely long wire equation 2.3.

$$B = \frac{\mu_0 I}{2\pi r} \tag{2.3}$$

Where I is the current in the wire and r is radial distance from the wire. According to equation (2.3) to obtain the 21.2 $_{\mu}$T required for 6.23mW output, a harvester located at 50cm from the conductor would need to have approximately 53A flowing through it.

If power consumption for every 12.7kW SWER customer was assumed to be 1kW (rather optimistic) this would equate to a continuous AC current of approximately 79mA from each customer. In reality, the current flowing through any particular part of the network is

determined by the summation of current drawn downstream, thus to obtain 6.23mW we would need approximately 671 customers downstream of a magnetic field harvester!

Another option proposed by Roscoe et al (2009) is to enclose the conductor with the secondary coil. Power output figures obtained from various different coils enclosing a conductor carrying 1A of current ranged from 0.06mW to 1.1mW. This limitation would still require many customers to be downstream of the device if it is to be provided with adequate power while noting that SWER networks only service between 10 to 50 customers each in total (Nous Group 2010). 'Threading' the power line conductor with the harvester also presents a problem but semi-enclosed 'clip on' devices have been proposed and warrant further investigation.

2.1.2.1 Summary

The relatively low and non-uniform current flowing through rural SWER lines is not expected to achieve the required power budget via magnetic field harvesting by any practical means. It is worth noting, however, that a current transformer may be needed in the proposed device for condition monitoring purposes, as opposed to power supply purposes, and as such could possibly be dual purpose.

2.1.3 Electric Field

Two conductors, such as a power line enclosed in a cylindrical electrode (Figure 2.2), will have a capacitance between them as described by equation 2.4. A second effective capacitance occurs between the electrode and the ground, as depicted in Figures 2.3 and 2.4. This system approximates a capacitive voltage divider between the conductor, the electrode and the ground as shown by the equivalent circuit (figure 2.3) and underpins the proposed works of Zhao et al (2012).

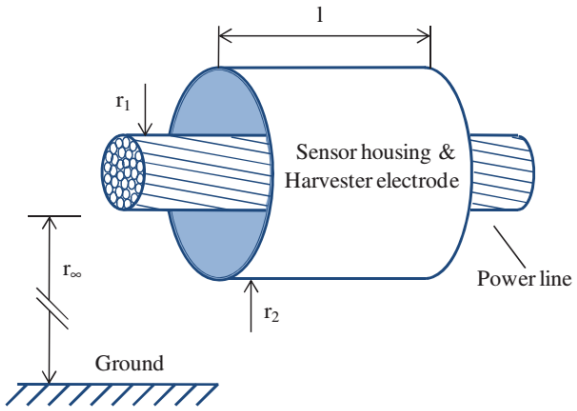

Figure 2.2 – Cylindrical electrode enclosing conductor (Keutel et al 2012)

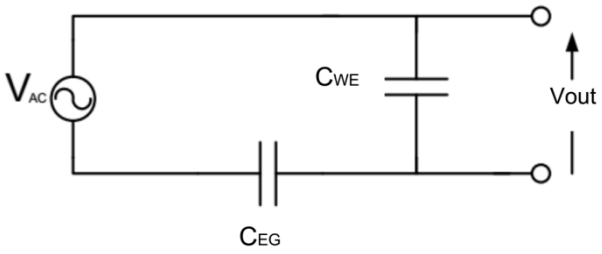

Figure 2.3 – Capacitive Divider (Keutel et al 2012)

The capacitance between the conductor and the cylindrical electrode can be approximated using the formula for capacitance per unit length of a coaxial system (Zhao et al 2012).

$$C_{WE} = \frac{2\pi\varepsilon_0\varepsilon_r l}{\ln\left(\frac{r_2}{r_1}\right)} \tag{2.4}$$

Where ε_r is the dielectric strength between the wire and electrode, l is the length of the harvester and r1 and r2 are the radii of the wire and cylinder respectively.

The capacitance between the cylinder and ground can be approximated using the formula below (Zhao et al 2012).

$$C_{EG} = \frac{2\pi\varepsilon_0 l}{\cosh^{-1}\left(\frac{h}{r_2}\right)} \tag{2.5}$$

Where h is the height above ground in meters.

The radial electric field associated with an energised wire conductor will result in a voltage difference across the plates according the capacitive voltage divider equation below.

$$V_{out} = V_{AC}\,(\frac{C_{EG}}{C_{EG} + C_{WE}}) \tag{2.6}$$

To extract the energy stored in the harvester capacitance C_{WE} , a load will need to be applied across it as shown in Figure 2.4 (Zhao 2012).

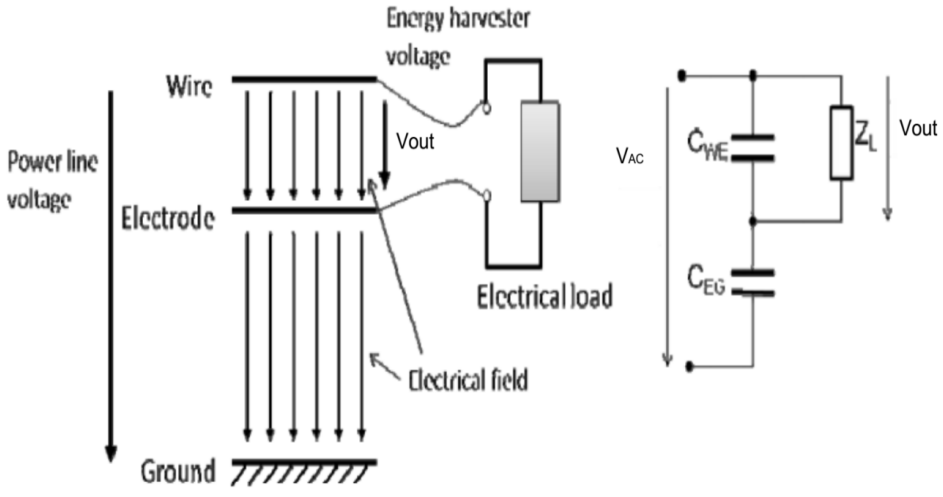

Figure 2.4 – Capacitive System with load (Zhao et al 2012)

Finding the voltage across the load requires the use of a general impedance voltage divider as shown below (Zhao et al 2012).

$$V_{out} = V_{AC}\left(\frac{\frac{Z_L}{1+j\omega C_{WE}Z_L}}{\frac{Z_L}{1+j\omega C_{WE}Z_L}+\frac{1}{j\omega C_{EG}}}\right) \tag{2.7}$$

Substituting (2.4) and (2.5) into (2.7) gives the equation (2.8) below (Zhao et al 2012).

$$V_{out} = V_{AC}\left(\frac{j\omega Z_L 2\pi\varepsilon_0 l \ln\left(\frac{r_2}{r1}\right)}{\ln\left(\frac{r_2}{r1}\right)\cosh^{-1}\left(\frac{\mathrm{h}}{r_2}\right)+j\omega Z_L 2\pi\varepsilon_0 l\left[\ln\left(\frac{r_2}{r1}\right)+\varepsilon_r\cosh^{-1}\left(\frac{\mathrm{h}}{r_2}\right)\right]}\right) \tag{2.8}$$

Real power dissipated in the load can be expressed as the following.

$$P = \frac{|V_{out}|^2}{Z_L} \tag{2.9}$$

Equations (2.8) and (2.9) were used by Zhao et al (2012) to estimate power outputs for various chosen parameters and by varying power line voltages and load resistances and simulating with Matlab. Power line voltages did not include the voltage of interest here (Victorian SWER 12.7kV) and so a similar exercise has been completed with the results shown below in Figure 2.5. Parameters were chosen to approximate the situation of a cylindrical harvester (length 30cm, radius 5cm, $\varepsilon_r = 1$) enclosing a SCGZ type conductor (radius 5mm) at a height of 7m energised to 12.7kV.

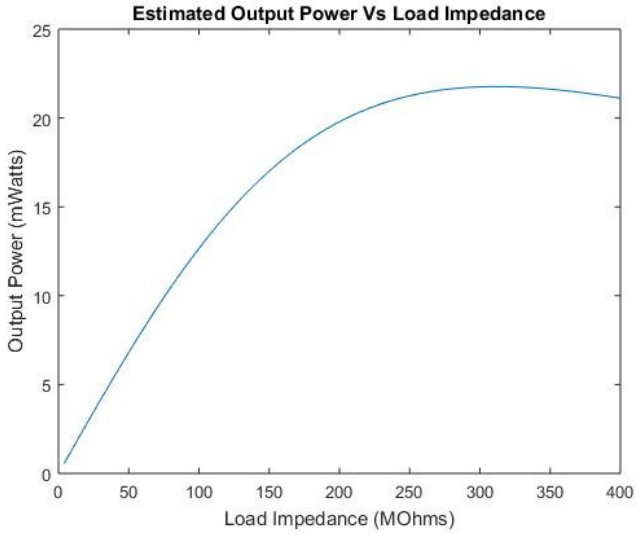

Figure 2.5 – Simulated Power Output for Electric Field Harvester with varying load impedance (Stephens 2016)

The topology described can be thought of as a voltage source (Vac), with very high source impedance effectively created from the very small capacitance to ground (C_{EG} equates to hundreds of MOhms at 50Hz). The simulation clearly shows a very high load impedance is required to obtain maximum power output which is expected. In this case the maximum power transfer occurs at approximately 300 MOhms. The voltage across the harvester capacitance will approach 1800V for a 300 MOhm load (as shown in Figure 2.6) and thus power conditioning will be need to be considered carefully given the fairly extreme parameters.

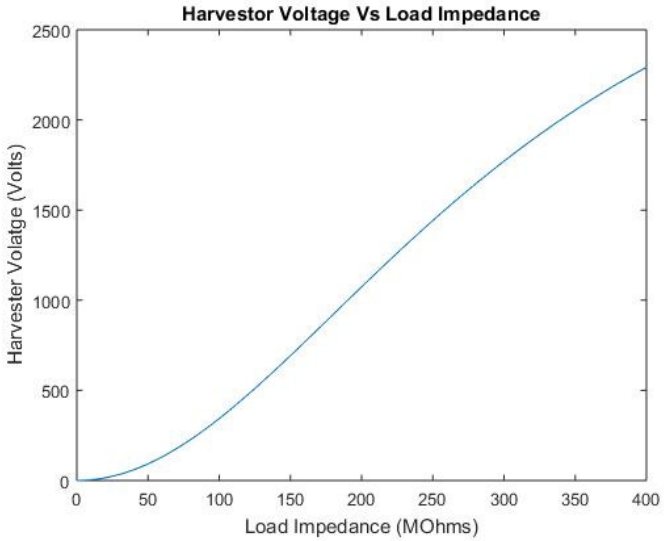

Figure 2.6 – Simulated Harvester Voltage for Electric Field harvesting with varying load impedance (Stephens 2016)

Rectification, impedance matching, voltage sensing, transforming and over voltage protection will need to occur in the subsequent circuitry before a load or battery can be connected.

2.1.3.1 Power Conditioning

To obtain a load impedance approaching that which is required, along with a useable voltage level, a voltage transformer may be utilised (Zangl et al 2009). A turns ratio of 120 in this case will yield $15V_{ac}$ at the secondary, along with presenting the capacitive voltage divider system with 300MOhm load if an approximately 21kOhm load is applied to the secondary, which is much more reasonable.

A method of accomplishing a static load is to utilise a shunt regulator (Zangl et al 2009). This will effectively cause the harvester voltage (V_{out}) to be clamped to a specific voltage, as determined by the shunt regulator applied to the transformer's secondary winding. Diode rectification may also be applied here.

High frequency Switching Converter topology methods have been proposed (Keutel et al 2012) but the added complexities involved in the required passive start-up and control circuits are not likely to be considered practical or reliable enough for this purpose.

Power conditioning for this technique is more involved due to compromises that need to be made between impedance matching of the load and source, and efficiency of circuits required to do so (Keutel et al 2012).

2.1.3.2 Power pole mounted devices

No research had been found that considers an electric field harvesting device that is not directly connected to the energised conductor. Considering the meagre power outputs estimated to be derived from electrodes effectively enclosing the conductor and thus cutting a large proportion of field lines, it is not expected that plates further removed from the conductor will yield useable results.

An electric field device that is not necessarily mounted on the actual conductor was proposed by Moghe et al (2009) in their comparison of energy harvesting techniques for power systems. The core of the device is a pair of rectangular plates acting as electrodes with one plate electrically connected to the power line conductor. The result is effectively another capacitive voltage divider but with C_{WE} and C_{EG} calculated according to equations (2.10) and (2.11).

$$C_{WE} = \frac{l^2 \varepsilon_r \varepsilon_0}{h} \tag{2.10}$$

$$C_{EG} = \frac{2\pi\varepsilon_0 l}{\ln\left(\frac{2\pi h}{l}\right)} \tag{2.11}$$

2.1.3.3 Summary

Essentially the electric field option for energy harvesting looks to be the most promising avenue for success to reliably and in every case fulfil the proposed device's energy budget. Like the case for magnetic induction energy harvesting, the harvester circuit itself should be considered as a convenient location to 'tap off' conductor signals for condition monitoring. A circuit function that provides periodic sampling along with a low voltage alarm/indicator is a likely scenario.

2.1.4 Piezoelectric

Significant research has recently gone into converting an alternating magnetic field to an electrical voltage via a vibrating piezoelectric cantilever, also known as magneto-electric conversion (Han et al 2015). Although power outputs are promising, the inherent mechanical vibration of such a device raises questions as to its life span and reliability. Typically these types of energy harvesting devices are more suited to micro sensors within industrial environments requiring small distances to transmit their data. Thus, power budgets required will likely be much smaller (10's of micro Watts) and unlikely to suit this project (Cantatore & Ouwerkerk 2006).

2.2 Communications

2.2.1 Introduction and Scope

To identify the areas of research that are relevant to the deployment of possible communications systems in the environment described in the section below. It is important to remember the aim of this project is to specify – but not fully design – the communications system.

In the wireless realm especially, the depth and breadth of communications research is very large. The field has branched out significantly, resulting in current research being more narrowly focused on sub-fields and specific applications. Broad, all-encompassing

'survey of technology' type articles such as the works from Akyildiz et al (2002) in 'A survey on Sensor Networks' are instructive, but cannot provide practical modern advice on wireless sensor network design due to the progression of technology since they were published.

Therefore, the approach taken was to seek out sources that may cover some of the relevant characteristics of this project's requirements. The characteristics, owing to their relatively demanding requirements, were seen to be the following:

- Range
- Power Consumption
- Reliability

These represent three critical design requirements, and the material presented in this chapter reflects that mentality.

A system of networked devices deployed on or near most power poles within one or more SWER line networks gives rise to specific requirements, options and limitations in regards to proposed communication schemes.

2.2.2 Device Deployment locations and range limitation

SWER suspension poles present possible convenient locations from which to deploy devices, either directly on the pole or clipped on to the adjacent conductor itself. Maximum spans between poles are quoted to be 380m for both ASCR/AC and SC/GZ conductor types (Parsons Brinckerhoff 2009) and even up to 1000m for special cases (Nous Group 2010). The extreme case of the 1000 meter span gives us our absolute minimum for device communications range; although this provides no redundancy should that link fail.

2.2.3 Base Station/Gateway Deployment Locations

Network isolation transformers that feed the circuit or automatic circuit reclosers (ACRs) that provide over current protection, may be convenient places to deploy a base station (communications gateway). The base station inter-connects with other utility communications systems such as wireless SCADA (supervisory control and data acquisition), WiMAX (Worldwide Interoperabilty of Wireless Access) or simply interfaces with the existing protection devices which will need to have remote control enabled. The base station will require much greater processing and communications capabilities and thus will need to be powered differently from the standard devices.

2.2.4 Data Traffic Requirements

The system requires a means to communicate urgent real-time fault detection warnings (event driven) as well as low priority periodic condition monitoring data (storage and forward). Both require information traffic to reach the base station in order for the information to be forwarded to their destinations. Both have very different requirements in terms of Quality of Service (QoS). Due to the information needing to be forwarded via multiple nodes, 'multi-hop' techniques must be used.

If periodic data is to be forwarded to the base station from all nodes (many to one) from the radially structured network, then it is clear that nodes closer to the base station will see more data throughput than others due the accumulation of forwarded data from the outlying nodes. Intuitively, these areas will define the minimum bandwidth requirements.

Another consideration will be the ability of the base station to send out messages for control, updates or possibly synchronisation messages to any or all nodes (one to many).

2.2.5 Reliability

It is important that the protection system of an electrical distribution network is highly reliable and robust. Communications presents as a possible weak link in a protection system, thus any communications network design must account for this.

Proposed is a system where reliability is enacted both through redundancy (inherent to mesh topology) and robust node design. Unfortunately, the area for the mesh to cover is large, and thus sensor density will be very low. The idea is that every node can communicate with no less than two nodes further upstream and two downstream, which effectively constitutes an 'N plus 1' redundancy scheme. This severely diminishes the mesh's ability to cover sensor loss such as is expected in a small scale, high density scheme (Akyildiz & Wang 2005) where many multiple paths are possible. It is therefore a requirement that the proposed devices themselves are sufficiently robust.

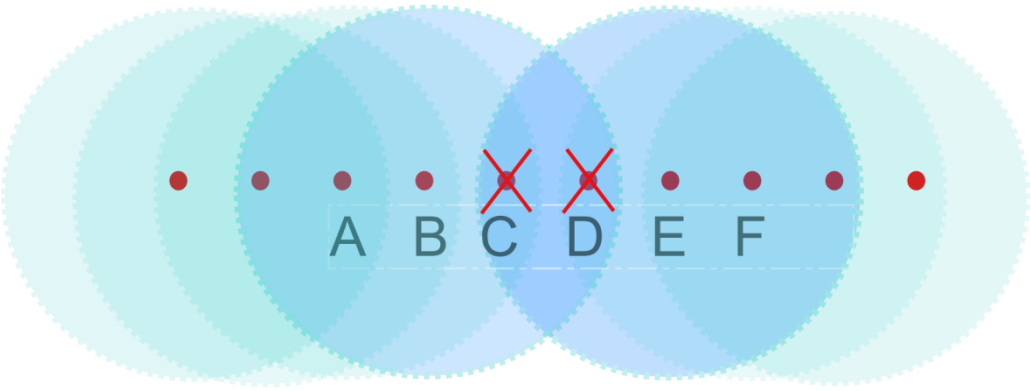

Figure 2.7 – Range and redundancy limit – two consecutive node failures in a straight line resulting in a broken partial mesh (Stephens 2016)

Figure 2.7 shows a theoretical straight line of wireless nodes with the ideal circular ranges of nodes B and E depicted. Any traffic either direction would only halt if both C and D drop out, as there is at least two paths present. Other alternative possibilities include using devices within range, deployed on other nearby power line strings or spurs to provide additional redundant paths; however, this cannot be relied upon.

Wired solutions are generally immune to this type of problem, but are impractical in this application given the installation costs. Power Line Communication (PLC) however, utilises the existing conductor and will be considered as an option. Given that powerlines are designed for power transmission and not data transmission, it would be likely that

communications transmitted along the conductor would require repeating. PLC can indeed be 'meshed' these days, according to Maxim Integrated (2012), which would effectively solve reliability problems with conventional PLC topologies. This being the case, then approaching the reliability problem with the above redundancy idea (inherent with mesh) is again relevant for PLC.

To enact a methodology like the one described requires each node to have at least double the range of the maximum span. Estimating this figure becomes more difficult for wireless sensors as terrain and other path loss mechanisms become a factor. Line of sight is basically guaranteed between consecutive poles, but for poles further away obstacles such as hills and vegetation will come into play.

2.2.6 Wireless sensor networks

Wireless sensor networks (WSNs) are a name given to a network of low power communicating devices. The functions of the devices (otherwise termed 'nodes') include:

- Communications
- Sensors / Actuators
- Processing
- Power Management

Figure 2.8 below is an adaption of the OSI network layer model presented by (Akyildiz et al 2002) which helps depict the extra 'parallel' layers that need to be considered for WSN design for all the regular layers. The model is not absolute, but provides a useful base for which to break down the node and network functions.

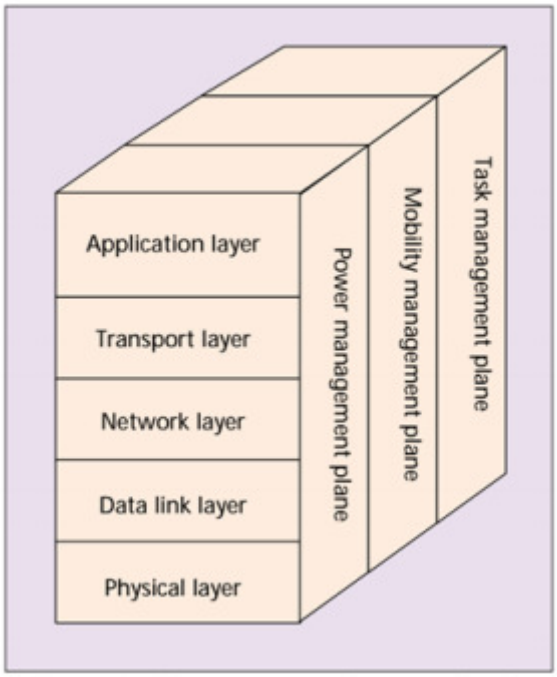

Figure 2.8 – Adaption of the OSI layer system for wireless sensors (Akyildiz et al 2002)

2.2.7 Physical Layer

This layer describes how transceivers transmit and receive emissions over the physical medium. Areas such as frequency selection, modulation techniques, spread spectrum techniques, and radio hardware are generally included here.

The proposed device has certain requirements that will likely require an in-depth analysis of this layer to achieve certain characteristics mainly to do with output power, sensitivity and power consumption during its different states (transmitting, receiving and idle).

2.2.7.1 RF Hardware

Modern WSN hardware technology is at a level where many components – transceiver, Processor, ADCs (analogue to digital converters) – can be found on single SoCs (system on chip) (Popovici et al 2013). Recently these modules have adapted the title ‘mote’, after the initial module called the Mica-Mote was designed by a group at University of

California, Berkley (Willis 2007). Willis (2007) performs an extensive review of many of the available motes on offer.

Due to the lack of range of existing motes, the design will likely need to select individual chips and combine to create a new type of mote that will serve the purpose, as has been achieved by Willis & Kikkert (2006)

Several transceivers, receivers, and RF Amplifier modules were compared for their power consumption information to help estimate power budget requirements for the communications module (Table 2.1).

Table 2.1 – Assorted RF chips with their power consumption attributes (Sourced from respective company datasheets)

Power Figures of Commercial RF Modules Examples						
Manufacturer	**Model/Type**	**Max Output (dBm)**	**Sensitivity (dbm)**	**Consumption**		
				Rx (mW)	**Tx (mW)**	**Idle (uW)**
Silicon Labs	Si4355 Receiver	N/A	-116	18	-	
HOPE RF Electronic	RF65W Receiver	N/A	-120	28.8	-	1.8
Chipcon	CC1000 Transceiver	10	-108	24.8	56	4.2
Texas Instruments	TRF37C73 RF Amplifier	18dB (GAIN)	N/A	-	182	413
Microchip	MRF89XAM9 Transceiver	10	-105	6.3	52.5	136

2.2.7.2 Frequency Selection

Industrial Scientific and Medical (ISM) bands are frequency bands used across the world for many and various applications that generally do not involve telecommunications and broadcasting. These are generally unlicensed bands throughout the spectrum and are defined for Australia by the Australian Communications and Media Authority (ACMA

2008). The ISM bands are not completely uniform across the world but include the following in Australia:

1. 6.780 MHz
2. 13.56 MHz
3. 27.12 MHz
4. 40.68 MHz
5. 915 MHz
6. 2.45 GHz
7. 5.8 GHz
8. 24.125 GHz
9. 61.25 GHz
10. 122.5 GHz
11. 245 GHz

Generally for regular far-field (wavelength smaller than distance) radio propagation requires antenna lengths with at least one quarter of the wavelength. As the frequency decreases the antennae size increases. Also as frequency increases, the signal loss associated with free space (FSPL) increases according to (eqn 2.12)

$$FSPL = \frac{(4\pi d)^2}{\lambda^2} \tag{2.12}$$

The ACMA (2008), through Australian legislation, also define the bandwidths and allowable emission power levels for particular bands and also the type of emissions (analogue modulation, digital modulation and frequency hopping methods etc). For the 40.68Mhz band the allowable EIRP (Equivalent Isotropically Radiated Power) is 1W for all transmitters, and in 915MHz is 1W for digitally modulated and frequency hopping transmitters and only 3mW for all others.

2.2.7.3 Modulation

Generally transceivers in wireless sensor nodes support simple modulation techniques such as on-off keying (OOK), frequency shift keying (FSK) and certain types of phase shift keying (PSK) (Willis 2007). The limitation here is the power required to enact more complex modulation – or even spread spectrum techniques – is not available. The higher data rates or higher channel efficiencies born from more elaborate modulations techniques such as 64-QAM are not required for most WSN cases, including for this project.

It is also noted that certain types of modulation that 'pass through the origin' are not appropriate for the Class 'C' type amplifiers used to provide efficient gain for the RF motes (Willis 2007).

2.2.7.4 RF power conserving hardware

Magno et al (2014) noted that in VLSI design it is widely accepted that asynchronous systems consume less power than synchronous systems. This idea is analogous to the mentality behind the design of a low power Wake Up Radio Receiver (WuR) which listens for specific asynchronous 'beacon' signals (using similar to OOK modulation) to tell the module to 'wake up'. The WuR module has the power to switch on other modules such as the transmitter or processor with extra low 'power gating' circuitry. The obvious advantage here is that the device can be listening in a low power state for long periods, saving energy. Unfortunately the WuRs exhibit relatively poor sensitivity an attribute also noted by (Ammar et al 2015). Surprisingly the power saving advantage offered by WuR is almost completely offset by the effective loss of receiving range especially if low level modulation techniques such FSK or OOK are already in use for regular communications.

2.2.8 Data – Link Layer

This layer defines how the physical layer is used (Medium Access Control, MAC) and thus will be very important in determining the energy consumption of the wireless communication. Traditional MAC protocols are not considered useful for WSNs because

they do not take into account energy conservation (Ullah & Kwak 2010). Also, protocols designs for WSNs are taking an 'information centric' rather than 'communication centric' approach to MAC and routing protocol design as it places more emphasis on the efficiency of communications (Popovici et al 2013).

The field of Wireless Body Area Networks (WBAN) is an area where power consumption is foremost in the mind of protocol designers, and as such may offer insight for other power sensitive applications of WSNs such as this one. A 'traffic adaptive' MAC protocol (TaMAC) is proposed by Ullah & Kwak (2010), which is intended to use beaconing or 'wake up' signals to prompt nodes to switch from a low power listening state to full power 'on' state.

Ullah & Kwak (2010) also recognised the problem that 'aggregate' type sensor networks have when many nodes detect the same event. A common event will cause many nodes to transmit at the same time, competing for the same medium and creating contention issues. Ullah & Kwak (2010) suggests that, from this viewpoint, contention-based protocols (such as CSMA) will be unsuitable for WBANs and may be similar for this project due to the scenario where a wire break fault will cause all downstream nodes to try and transmit the fault indication at the same time.

A distributed version of Time Division Multiple Access (TDMA) called SMACS (Self Organising Medium Access Control for Sensor Networks) is also considered useful for WSNs (Akyildiz et al 2002). TDMA is a synchronous method of nodes accessing the medium, upon which time slots are assigned. The duty cycle of which may be alterable to such an extent that power may be significantly conserved. This method will incur greater transmission delays (latency) however especially for 'round trip' traffic where the node delays will become accumulative.

FDMA (Frequency Division Multiple Access) is considered to require a hardware complexity that is too great to install on small low power motes (Willis 2007). Other hybrid approaches, including applications of CDMA (Coded Division Medium Access), require further investigating.

An analogous approach to Srbinovski et al (2015) energy aware adaptive sampling could be implemented in possible new TDMA based MAC designs and possibly exist already. The idea here is that input from energy harvesting function is fed to a dynamic MAC protocol, which can alter the duty cycle among other things that generally govern the transceiver activity.

2.2.9 Network Layer

The Network Layer is primarily concerned with routing methods and protocols. Routing for this project is unlikely to be a critical factor given the low data rates and lack of alternate routes to choose from. There are many routing protocols that are applicable to WSNs, and it is noted that some algorithms have been developed to be energy conscious in terms of routing (Willis 2007 & Akyildiz et al 2002).

This layer does however present opportunities to augment medium access control protocols such as TDMA so that methods may be introduced to decrease over all round trip propagation delays such as 'Spatial Re-Use' where simultaneous transmissions can occur between pairs of nodes that do not conflict (not within range of each other) (Djukic & Valaee 2007).

Implementation of security arrangements are also expected to occur at this level where authentication (ability to discern who the transmitter is) being the primary goal.

2.2.10 Transport and Application Layers

These layers are not considered layers that warrant extensive research in WSNs just yet, likely due to the amount of variations in the lower layers.

For this project, the application layer will represent the area where an onboard alarm detection algorithm interacts with alarm indication transmissions etc. Also SWER network node mapping – identification, location coordinates and possible integration of a GPS module – could occur as defined by this region, rather than as a function of the main program.

2.2.11 Mesh Networks

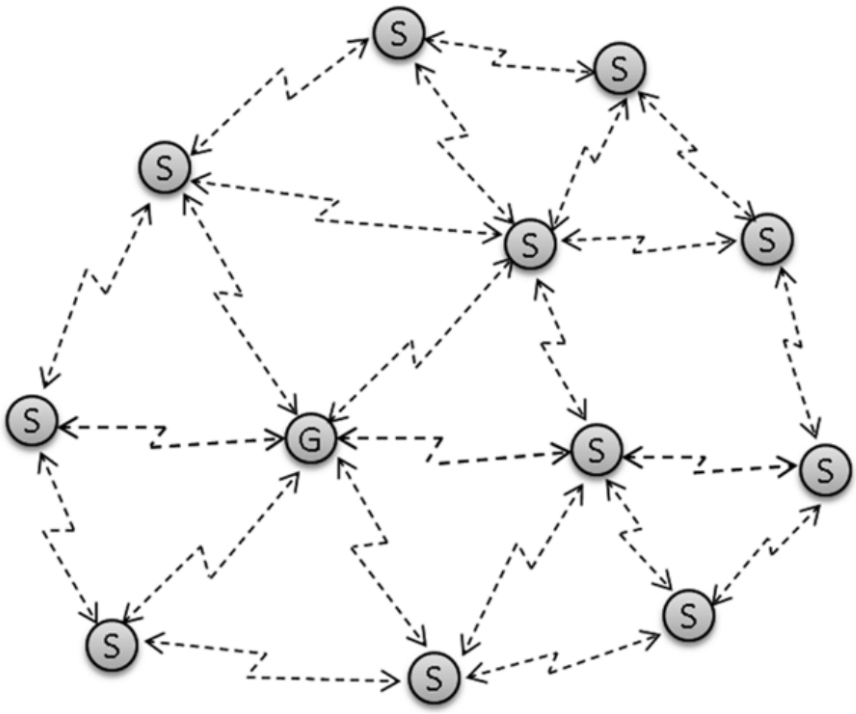

Figure 2.9 – Mesh Topology (Cecilio & Furtado 2014)

Mesh networks attempt in various methods to ensure every node can communicate with any other nodes within its range. A core function of mesh networks is to be aware of multiple paths between source and destinations, and to enact a path change when linking nodes drop out (Cecilio & Furtado 2014). Essentially, the system becomes 'self organising' and 'self healing' to some extent, and the number of paths are only limited by the number of nodes that can 'see' each other (Figure 2.9). This topology will be the only topology considered in this project.

2.2.12 Hybrid Topologies

Topologies that make use of more than one type to create a network are called hybrid topologies. Mesh and star topologies have been combined to take advantages of each – e.g. self healing of mesh, and simplicity of the star. The idea of a Wireless Mesh Network (WMN) having gateways to an infrastructure backbone is described as one type of WMN by Akyildiz and Wang (2005), and could be argued to be a hybrid topology just across different technologies.

As any two SWER networks will unlikely be similar, it is expected by the author that to apply hybrid topologies to all different SWER networks would be too difficult and time consuming to be practical. An infrastructure backbone would likely require a wired communications link that spanned the entire network; again, this is clearly not practical.

2.2.13 Wireless Mesh Networks

Wireless Mesh Networks (WMNs) is an ongoing research area in itself. It represents a dynamic system whereby where nodes can join and leave with peer to peer links made and broken automatically (Akyildiz et al 2005). It can also be thought of as a group of wireless routers operating in ad-hoc mode, with dedicated Medium Access Control and Routing Protocols to enact the mesh network.

Akyildiz and Wang (2005) points out Industry standards groups IEEE802.11, IEEE802.15 and IEEE802.16 have all contributed to WMN research and protocol standards design (Table 2.2). The research continues to attract a lot of attention, with many different MAC and routing protocols being designed for an expanding number of WMN applications.

Table 2.2 – Mesh Protocols Examples

Protocol Families Contributing to Mesh Systems		
Industry Standard Group	**Network Classification**	**Familiar Protocol families associated with these standards**
IEEE 802.11	Local Area Networks, Medium Area Networks	Wi-Fi
IEEE 802.15	Wireless Personal Area Networks	Bluetooth, Zigbee
IEEE 802.16	Wireless Medium Area Networks	WiMAX

Vast differences in network requirements and deployments of WMNs have led to many approaches to design and implementation. It was suggested by Parth & Dutta (2011) that a 'joint design approach' is likely required for WMN designers, who are invariably attempting to deal with multiple competing attributes such as: performance, band width, latency, jitter, reliability, power consumption, range, mobility, and quality of service. A regular problem is that existing protocols will satisfy some but not all of their criteria, making appropriate selections difficult.

Wireless Sensor Networks operating in a mesh topology constitute a sub set of WMNs and are afflicted by the same intractable design problems. Unfortunately these can be augmented further as Wireless Sensor Networks WSNs is a research area in itself and does not necessarily infer a mesh topology.

Some families of Protocols that are applicable to modern Wireless Mesh Sensor Networks were identified by Alcaraz and Lopez (2010)

- Wireless HART HCF
- 802.15.4
- 802.15.5
- Zigbee Pro
- ISA 100.11a

IEEE 802.16 standards (such as WiMax) seem more appropriate to a wider area mesh network due to the greater independence of nodes to operate without a dedicated backbone network as is the case with the proposed system. WiMax itself is a subscription based system with much higher power and complexity requirements and is not recommended for this application.

2.2.14 Range and radio propagation

According to the Friis transmission equation (eqns 2.13 & 2.14) the power at a receiver distance 'd' from a transmitter is obtained for ideal (free space) emissions (Grini 2006).

$$P_r = \frac{P_t \lambda^2 G_t G_r}{16\pi^2 d^2} \tag{2.13}$$

Where P_t and P_r are the transmitted and received power figures, G_t and G_r are the respective gains for isotropic radiated type (non directional) antennas and λ is the wavelength. For use with figures in log ratios equation 2.14 can be used.

$$P_r = P_t + G_t + G_r + 20\log\left(\frac{\lambda}{4\pi}\right) - 20\log(d) \tag{2.14}$$

This equation is useful with radio and antenna design to estimate the minimum link budget (P_t . P_r) required to achieve a required range. In general the figure obtained will be much lower than is actually needed due to a number of factors contributing to path loss not being accounted for in this equation.

A rule of thumb to help designers include path loss proffered by Chipcon and Texas Instruments in various application notes and states (Grini 2006):

- *120db link budget is needed at 433Mhz to achieve 2000m*
- *Plus 6db doubles this distance*
- *Double the frequency – half the range*

This is basically adding approximately 28dB to the link budget figure obtained in equation 2.14 to account for any number of real world circumstances. This will be useful for 'ball park' type calculations, but further analysis would be required if more accurate modelling is needed and environmental conditions are known.

Effects contributing to path loss can be caused by terrain, obstacles, reflections (multiple paths), refraction (atmosphere and curved earth effects), diffractions (radiation scatter by obstacles) and antenna heights (Willis 2007). BER (bit error rate) and transceiver noise figures also need to be taken into account when attempting to define a maximum range.

For the situation involving devices deployed at or near the top of consecutive 12 meter high power poles having line of sight with each other, the problem of modelling the radio propagation should not be a strenuous one. The main effects will be attributed to by the vegetation either side of the cleared power line route, and the ground itself. Possible solutions to model this situation could utilise The Two Ray model for line of sight conditions and the Plane-Earth model for low lying antennas (Willis 2007).

For devices deployed on non consecutive power poles it is likely vegetation and non line of sight problems will be encountered. According to McLarnon (2005), a forest will cause 0.4dB/m at 3GHz, 0.1dB/m at 1GHz and 0.05dB/m at 200Mhz and using these figures some measure of degradation to the link budget could be immediately obtained.

As ranges usually less than 1Km it will be unlikely that more than one or two hills or valleys will separate transmitter and receiver, and thus it may be adequate to use diffraction loss formulas based on single obstacles found on the path. The Dougherty and Malony formula can be used for rounded obstacles or the Fresnel Integral for knife edge obstructions. Alternatively more complete computer models such as ITM (Irregular Terrain Model) or the PTP (Point to Point model) to give a more general view of expected field strengths in the area after providing a range of environmental parameters to the computer program (Willis 2007).

2.2.15 Long Range Wireless Sensor Networks

Some research has gone into long range wireless sensor networks including (Willis 2007) from James Cook University whose main objective was to *'investigate what changes are required to existing wireless sensor nodes to allow long-range communications'*.

Willis (2007) project addresses the need for long range wireless networks (LRWSN) in large areas of land that are commonly encountered in the Australian landscape. The study briefly surveys the existing wireless sensor protocols and technologies currently available, and then discusses and develops appropriate radio propagation models for various applications.

A hardware prototype was designed for use in the 40MHz ISM band. The device was called the JCUmote and was developed from the adaption of existing device called the Mica2. CSMA/CA and MintRoute were used as the data-link and network layers respectively and the sensor processor was installed with the TinyOS operating system which is effectively a cut down version of Linux.

The test was reported largely successful in demonstrating an operational Wireless sensor network over long range in a variety of landscapes. The sensor nodes deployed had ranges over 10Km, but were not subjected to the same power and antenna constraints as this project nor was the network completely 'meshed'.

2.2.16 Security

Powerlines are important infrastructure providing an essential service to the public. By its nature, a wireless system is more prone to interference from third parties than that of wired alternative due to the medium of transmission being open to anyone within range. Ad-hoc type networks are inherently more difficult again to enact security due to the high constraints it places upon sensor node hardware (Alcaraz & Lopez 2010). Alcaraz and Lopez (2010) provide a security analysis upon Wireless Mesh Sensor Networks.

Security of wireless mesh communications systems is an area of research that is ongoing and not at all mature nor does a consensus agree on how to approach it. For this reason it will be considered out of scope for this paper, but by no means can it be left out of any

design considerations and will indeed need to be designed into the system from the ground up.

2.2.17 Power line communications (PLC)

Recent advances in Power line communication resulting in new protocol 'G3-PLC' by Maxim Integrated being developed, are opening up the possibility for the relatively old technology to be 'meshed' (Maxim Integrated, 2012). G3-PLC uses orthogonal frequency division multiplexing (OFDM) with enhanced error correcting facilities to enable data rates fast enough – quoted up to 300kbps – to contend with the amount of 'message forwarding' and 'two way communication' that occurs with meshed networks.

It was noted by Kikkert and Reid (2009) in a report on PLC and BPL (Broadband over Powerlines) that SWER lines in particular were not suitable for BPL applications due to the SWER line's transmission characteristics being unable to support frequencies up into the MHz region. PLC (which used up to 200kHz) was deemed to be OK for SWER but the report predates the release of G3-PLC. Data on the G3-PLC MAX2992 transceiver from Maxim Integrated indicates an operating frequency of 10Hz to 490kHz. Gay et al (2009) considered condition monitoring using PLC for SWER to be feasible and noted that PLC frequencies can reach up to 500kHz plus, inadvertently lending support to the notion that G3-PLC will work on SWER.

The technology is mainly focussed on meter reading applications but may be applicable for this project given that the proposed devices may well need to be deployed directly on to the conductor. Power consumption may be prohibitively high however (possibly into hundreds of mW) to be used with the proposed energy harvesting options.

2.3 Fault Detection

2.3.1 Existing Fault Protection

Protection schemes for the Victorian SWER lines typically used Oil filled Circuit Reclosers (OCRs) situated at points that essentially divide the individual SWER line networks into protected sections. The OCRs are manually set, i.e. with no remote communications, and can be adjusted to open the circuit once a specific over-current

condition is exceeded (Holmes 2011). The reclose setting can be adjusted – also manually set – to set the number of and timing of reclose attempts. ACRs have the ability to be set remotely and provide similar functionality to OCRs but provide for greater sensitivity and faster response times (Holmes 2011). They can utilise SCADA systems to remotely reprogram the devices, and this presents a possible avenue for interface with future technologies.

Some variants of new generation ACRs utilise the IEC 61850 communications protocol/standard, providing an even greater possibility of integration for this project.

2.3.2 High Impedance Earth Faults and Arcing

When an energised conductor contacts an object that is in contact with the ground, the object provides a path for the current to flow to earth. The object will have a certain resistance or impedance that restricts that flow. A tree branch or other low conducting materials will have high impedance and thus the fault current may not be enough to trip any over current protection present on the line. This scenario is generally what is deemed to be a high impedance earth fault.

Upon the conductor first striking the high impedance object, arcing will often result. Often the strike will not be 'clean' and many strikes will occur, causing multiple arcs. Even when the conductor and object has physically settled, the contact between the two is often not adequate enough to pass electricity without some arcing between them.

The arcing can identify itself as a high frequency voltage 'spike' or RF transient on the conductor, and could be detected for a certain length down the line depending upon the magnitude before intrinsic characteristics of the line, i.e. line inductance, start to filter it out. The nature of the poor connection between the conductor and grounded object gives rise to an intermittent conduction scenario which also adds to the earth fault signature. Due to the highly variant nature of HIFs and load profiles, these faults are difficult to detect effectively. Many methods have been tried in the past, with no single method being found to cover all possible scenarios and, in some instances, no methods have been found effective (Kawady et al 2010).

For HIFs to ignite a fire, arcing is generally required to be present thus detection of the arcing itself could present an opportunity to protect against bushfire ignition. According to Kawady et al (2010) there are three main approaches for detecting arcing:

- *Frequency domain methods where periodic fourier transforms are applied to current and voltage signals and compared to known arcing spectral signatures*
- *Time domain methods which compare certain aspects of voltage and current waveforms to known arcing waveform signatures*
- *Non conventional methods such as wavelet analysis where tine and frequency domains are plotted against each other and compared against known arcing signatures for this realm.*

All of these techniques involve analysing the current or voltage waveforms or subsequent spectral components to try to detect signatures of arcing. Unfortunately these signatures will also appear different when various types of loads are present on the line. Complicating matters further is the fact that modern power electronics such as inverters and motor controls can exhibit signatures similar to certain HIFs due to their non linear and high frequency current draw that are also attributes of arc currents (Kawady et al 2010).

Much of the literature reviewed to date in this area has focused on source-side or load-side monitoring and detection (Djuric & Terzija 1995). The nature of this project is to have multiple points of monitoring across the network and thus it may be possible to achieve better results having possible faults closer to the detection device as well as having the ability to differentiate between other nearby devices. The location of the fault itself may even be possible using spread spectrum time domain reflectometry (Smith et al 2005).

In Holland's (2013) summary of possible high impedance fault detection techniques for SWER, Holland includes methods involving measurements of the third harmonic current phase angle with respect to the primary voltage waveform, other waveform signature based techniques and an open conductor detection system such as the one proposed.

For this project it is proposed that devices simultaneously monitor current flow as well as voltage. More sophisticated fault detection may then be made possible using both the data

streams using logic and ‘sum and difference’ techniques using nodal analysis incorporating Kirchhoff’s Current Law (KCL).

2.3.3 Network device mapping

Any usable fault detection system of the nature proposed will require that the system as a whole is ‘aware’ of the orientation of the network, and the relative and absolute locations (GPS co-ordinates) of all the devices. This will be for two fold reasons.

a) To determine where faults are located by comparing adjacent nodes data

b) To notify the maintenance crews of the area in which the fault lies

This is not an area that has attracted significant research due to the highly specific application being dealt with.

2.4 Summary

Presented are investigations into communications, power harvesting, fault detection and over-all system research areas. Initial findings reveal the most promising technologies and methodologies that should be investigated further for their application to this project.

A summary is compiled in Table 2.3 below.

Table 2.3 – Summary of Technologies Reviewed

Technology	Comments
Energy Harvesting	
Electrostatic Harvesting	Primary method to investigate, possibility of 10's of milli Watts
Magnetic Induction Harvesting	Alternative method, probable insufficient current flow in conductor
Piezoelectric Harvesting	Mechanical vibration a disadvantage, added complexity and low output
Communications	
Hardware	Focus on low power consumption modules with simple modulation techniques
Medium Access Control	Ability to deal with contention and guaranteed Quality of Service required. TDMA methods look promising
Mesh	Methods complying with IEEE801.16 seem most suitable
Fault detection	
Arc Detection	Difficult to differentiate between normal loads and arcing faults
Open Conductor Logic	Simple and effective approach however does not capture all HIFs
Wavelet analysis	Computational overheads seem prohibitive for small low powered devices

3 Methodology for Energy Harvesting

3.1 Introduction and Scope

The general theories to be verified in this project are as follows:

A power budget sufficient for all functional requirements of the individual device can be obtained from the SWER line conductor by utilising energy harvesting techniques such as magnetic induction and electrostatic methods.

The detection mechanism will be actuated by a strategy that identifies devices as nodes of a network. If a fault such as a line break occurs somewhere on the network, devices (nodes) downstream of this break will lose power. By making a series of comparisons between nodes' input power, the system will be able to reliably detect line breaks and possibly even other earth faults.

The general methods by which these theories are to be tested are the following:

- Design, model, build and test an energy harvesting prototype that utilises either electrostatic or magnetic induction techniques, or both, to help provide data and understanding on deriving power from the conductor of 12.7kV SWER lines. The prototype will be a scaled 0- 240V, 0 -10A version of the live conductor (this method is expected to provide directly relevant data for magnetic induction techniques but be only moderately relevant to electrostatic techniques; a 12.7kV experiment is out of the scope for this project). The primary experiment however will concentrate on the electrostatic technique due it exhibiting the most promising method of energy harvest in the 12.7kV SWER situation.

- Design the overall system operating mechanism via software algorithms and visual aids (interactive flow charts), simulate and test scenarios. Demonstrate how the system can determine a genuine fault and discriminate against all other normal operating conditions.

- Design the overall device to a level so that the power budget can be accurately determined, as well as exploring other possible limitations to do with reliability, complexity, implementation and cost.
- Research and propose other methods that could detect earth faults on SWER networks such as detection of the accompanying high frequency arcing.

3.2 Electrostatic Energy Harvesting Experiment

3.2.1 Experiment Aims

- Create and test a simulation model that will be used to easily test changes in physical parameters in the design of the 12.7kV SWER design version. The model will be audited against the 240V electrostatic physical experiment.
- Determine practical limits that prohibit certain aspects of physical designs.
- Identify physical components that affect the system not taken into account in the model.
- Ultimately help to identify a reasonably accurate power budget figure that would be realised for a 12.7kV SWER design installation.

3.2.2 Simulation Model

The general schematic of the electrostatic energy harvester is shown in figure 3.1. The design is based on ideas presented by Zangl (2009) and Zhao (2012). Both examples use a cylindrical conductive electrode that surrounds the conductor (C1) which presents one half of a capacitive voltage divider (the other half is between the electrode and ground (C2)). Both also use a transformer to help match impedances between the load (energy storage circuit) and the source.

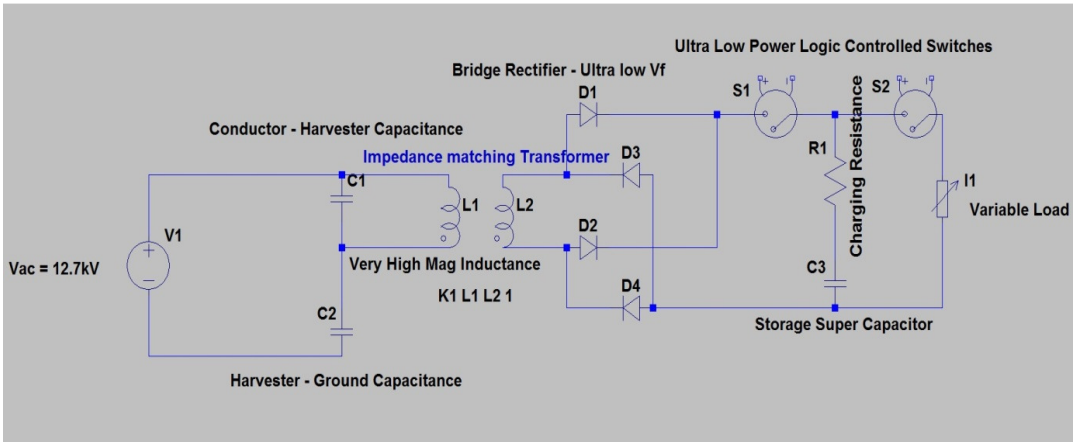

Figure 3.1 – Electrostatic energy harvester schematic (adaption of circuit design by Zangl 2009)

The transformer itself can significantly load the harvesting device if the primary magnetising inductance is not very high (in the range of kilo-Henries). The significant impedances as seen by the harvester are depicted in the equivalent circuit shown in Figure 3.2.

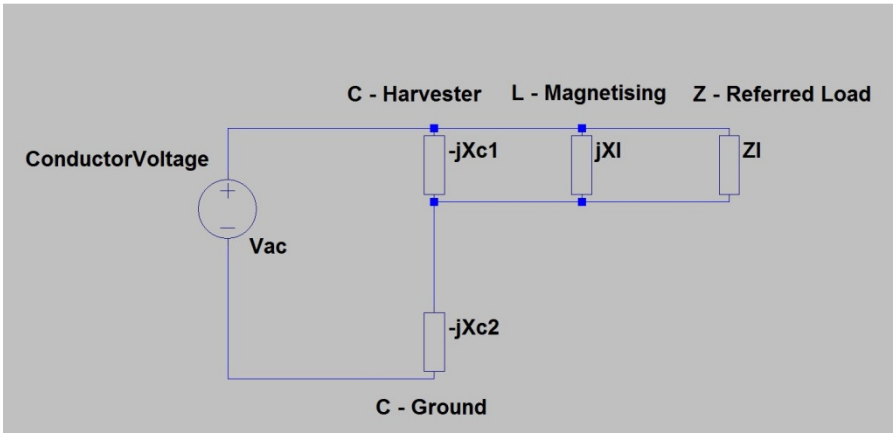

Figure 3.2 – Equivalent AC reactances encountered by the harvester (Stephens 2016)

The transformer primary voltage is thus affected by the four major impedances present as depicted. This equivalent circuit is used in the model to initially determine the transformer secondary voltage which in turn can be used to determine the final DC

storage capacitor voltage (after rectification). This voltage will be used with the Thevenin equivalent DC resistances as seen by the storage capacitor to then determine the RC charging time constant (see Figure 3.3).

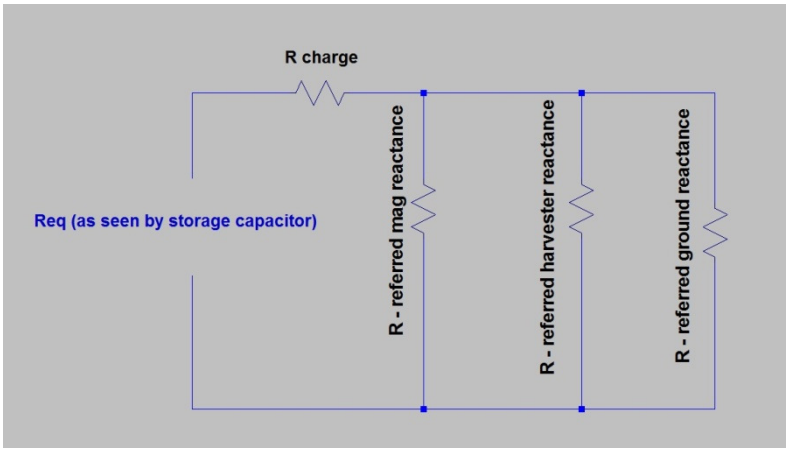

Figure 3.3 – Thevenin equivalent DC resistances as seen by the storage capacitor (Stephens 2016)

Once the time constant is determined charging times can be determined and thus average power outputs found from the charge stored in the capacitor.

The equations used are:

$$V_{storage} = V_{Final} - V_{Final}\ x\ e^{\frac{-t}{R_{eq}xC_{storage}}} \tag{3.1}$$

$$W_{stored}\ (Joules) = 0.5xC_{storage}\ x\ V_{storage}^2 \tag{3.2}$$

$$P_{average}(Watts) = \frac{W_{Final} - W_{Initial}}{t_{Final} - t_{Initial}} \tag{3.3}$$

The code for the Matlab model can be found in Appendix D.

3.2.3 Simulation Scenarios and Results

To help verify the model, it was run after being provided with parameters matching that of Zangl (2009) and Zhao (2012)'s experiments. The results were convincing of the models legitimacy. The model was then run to simulate the 12.7kV SWER and 240V mains situations.

It was noted that power could be increased significantly if was calculated using only the charging voltage of up to approximately only 1 time constant where the charging slope is greatest. This could conceivably be realised with practical circuits if the capacitor storage voltage was still high enough to be utilised. The power for normal and low cut-off storage capacitor voltage figures are shown in Table 3.1 along with the storage capacitor charging voltage waveforms. For all other input parameters used and outputs for all simulations see Appendix E.

Table 3.1 – Simulated Power Outputs (parameters gleaned from Zangl 2009 & Zhao 2012 experiment and put through Stephens 2016 simulation model)

Simulation	Conductor AC Voltage	Power Output – Measured / Quoted (mW)	Power Output – Simulated (mW)	Power Output – Simulated using lower cut-off Vsc (mW)
Zangl	150000	370	229.5	344.8
Zhao	60000	16.4	14	21.6
SWER	12700	-	2.8	4.3
Mains	240	-	.0063	0.009

Limitations of the Zangl and Zhao simulations arise from as number of parameters being unknown. The major unknowns were the relative permittivity of the harvester capacitance, the magnetising inductance of the transformer and the actual storage circuit and measurement technique used to take the energy and power measurements.

Parameters used for the 12.7kV and 240V Mains systems were kept as similar as possible to for model verification purposes. According to the model, outputs for the 12.7kV SWER and 240V mains systems could be boosted significantly to 18.6mW and 60uW

respectively simply by adding a polystyrene dielectric to the energy harvester capacitance (Figures 3.4 to 3.7).

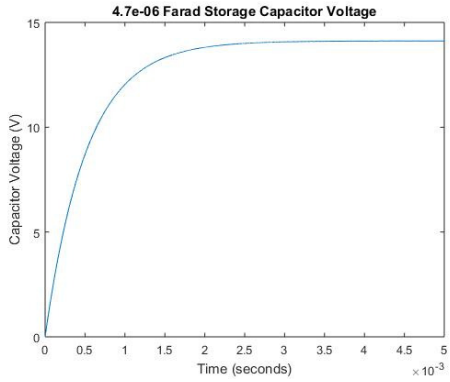

Figure 3.4 A – Normal (Stephens 2016)

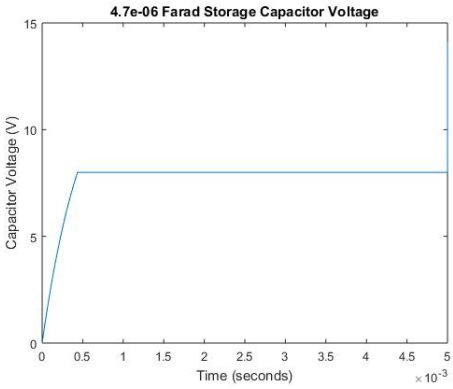

Figure 3.4 B – Low cut-off voltage using maximum slope for charging only (Stephens 2016)

Note: Both simulations run using parameters in Zangl's experiment – found in Appendix D

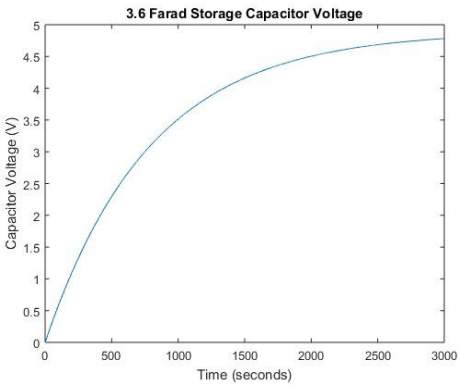

Figure 3.5 A – Normal (Stephens 2016)

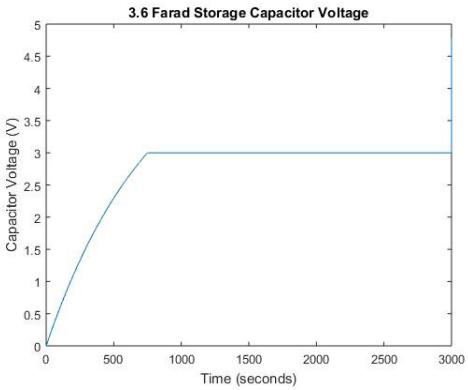

Figure 3.5 B – Low cut-off voltage using maximum slope for charging only (Stephens 2016)

Note: Both simulations run using parameters in Zhao's experiment – found in Appendix D

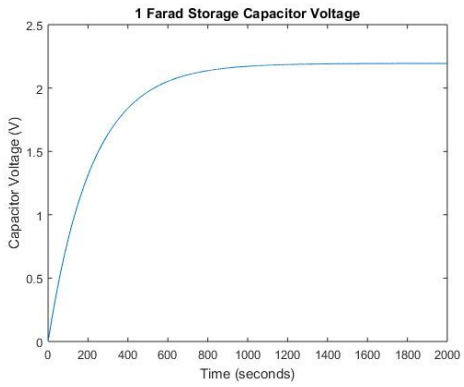

Figure 3.6 A – Normal (Stephens 2016)

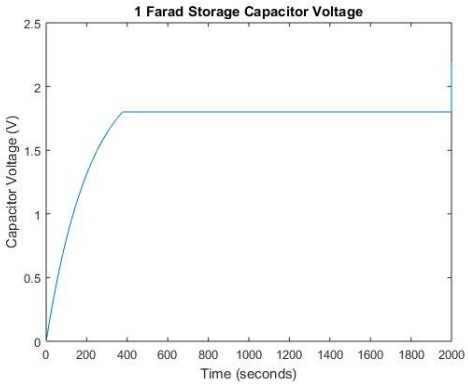

Figure 3.6 B – Low cut-off voltage using maximum slope for charging only (Stephens 2016)

Note: Both simulations for 12.7kV SWER – parameters can be found in Appendix D

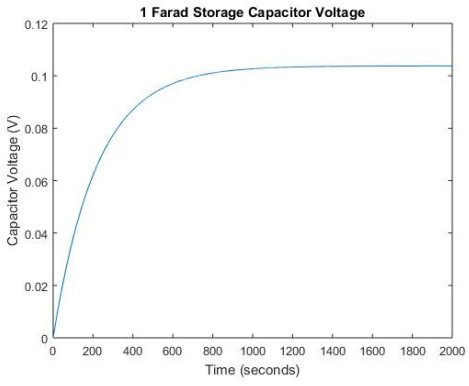

Figure 3.7 A – Normal (Stephens 2016)

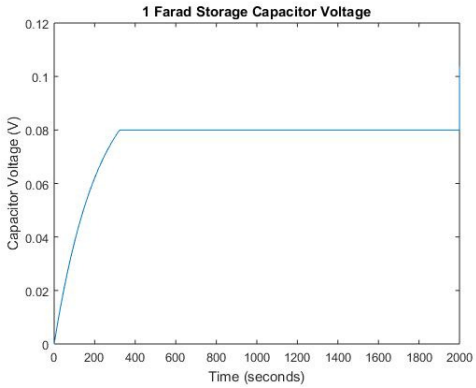

Figure 3.7 B – Low cut-off voltage using maximum slope for charging only (Stephens 2016)

Note: Both simulations for 240V Mains – parameters can be found in Appendix D

3.2.4 Final Designs

The final designs take into account practicalities of the 240V RMS scenario. It is understood that due to the magnetising impedance of the step down transformer (featuring in Figure 3.8) being an unknown quantity (before procurement at least) and likely being a significant burden on the harvester, a second experiment will take place that forgoes it completely in an attempt to quantify its effect on power transfer (Figure 3.9). Also of concern is the possibility that with zero initial voltage on the storage capacitor (presents as a short) the impedance will be so low as to inhibit the diodes from switching on, thus no current will flow causing no charge to build up on the capacitor.

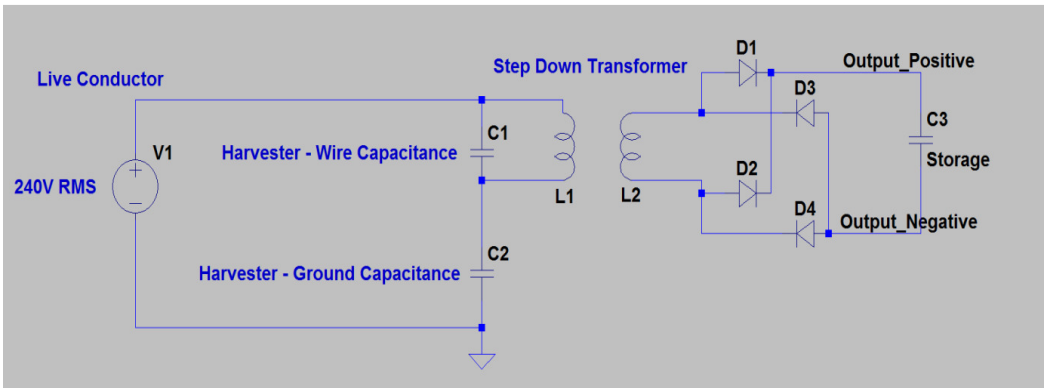

Figure 3.8 – Initial Circuit – Step down transformer included (circuit adapted from Zangl 2009)

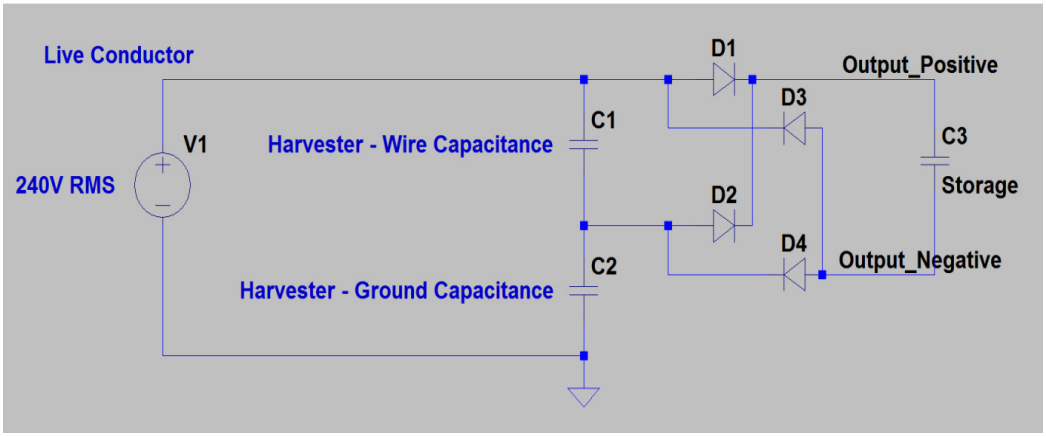

Figure 3.9 – Second Circuit – Step down transformer removed (circuit adapted from Zangl 2009)

Another practical issue of concern is the effect of measuring equipment loading down the circuits under test. This is expected to be significant due to the relatively low input impedance of the 'Meterman 38XR' chosen to perform the real time voltage measurements across the storage capacitor. Due to the very high effective source impedance presented by the ground to harvester capacitance, a large portion of the very small current being supplied will be shunted through the meter instead of charging the capacitor, and at the same time placing a large effect on the voltage divider resulting in a much smaller voltage across the harvester electrodes. This in turn will clearly limit the final charging voltage available to the storage capacitor.

This problem will be accounted for in two ways:

1. Measure the meter's input impedance before taking measurements and include in the subsequent power calculations
2. Conduct subsequent experiments without the meter and test after periods of charging, making sure the storage capacitor has a value large enough to ensure reasonably accurate readings that would otherwise be obscured by rapid discharging through meter.

3.2.5 Lab Experiment

A 27cm long aluminium cylinder with a radius of 3.75cm was acquired and prepared to be suspended via insulating material to a taut copper insulated wire (Figure 3.10). It was decided that the wire need not be stripped of insulation as the contribution to the relative permittivity to the conductor – harvester capacitance was considered negligible (free air is used as the 'dielectric' as this will assist achieving a lower capacitance which is desirable as it will shunt less current away from the storage capacitor simultaneously causing a greater voltage drop across it for harvesting).

A virtual ground plane was constructed from conductive sheet metal (Figure 3.11) and was fixed beneath the suspended harvester. The area was cleared as much as possible from other conducting objects including the ground to minimise other stray capacitances but this was not perfect considering mains cables were present to provide supply and were also hardwired in the vicinity.

Figure 3.10 – Electric field energy harvesting experiment apparatus (Stephens 2016)

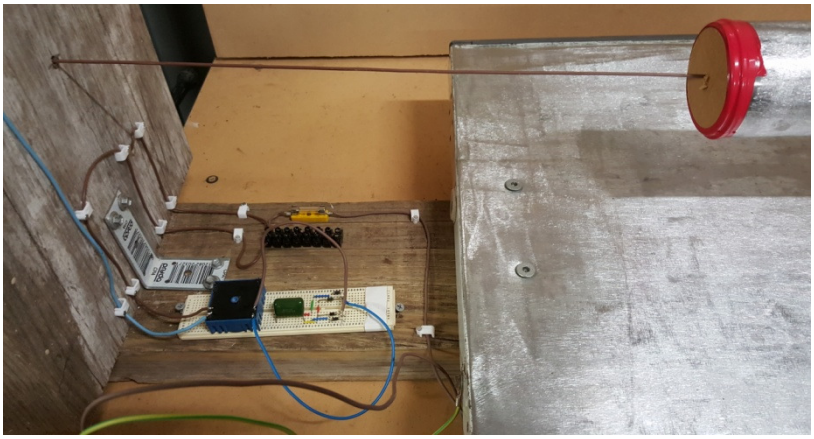

Figure 3.11 – Electric field energy harvesting experiment close up including transformer (Stephens 2016)

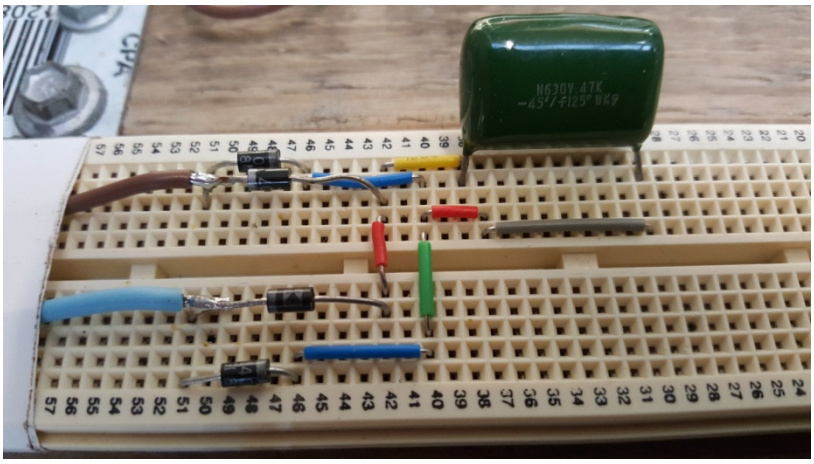

Figure 3.12 – Electric field energy harvesting experiment close up of charging circuit with transformer omitted (Stephens 2016)

The Meterman 38XR multimeter input impedance measured to be approximately 9.16 Mega Ohms via its contribution to a resistive voltage divider combination with a 1.21 Mega Ohm resistor.

The transformer (Figure 3.13) magnetising impedance was measured by inserting the primary, then secondary, into a voltage divider circuit driven from a regular 12V, 50 Hertz AC voltage source. The winding resistance was considered negligible and thus all current flowing threw it was considered reactive. This was basically a pseudo 'no load' transformer test but without the power meter to measure the power factor as one was not available. Transformer magnetising impedance or 'self inductances' were measured to be:

- Primary – 14.12V across and 45uA through yielding 313.78 kOhms (988.7 Henries)
- Secondary -8.18 V across and 590uA through yielding 13.86 kOhms (44.1 Henries)

Figure 3.13 – Transformer with high magnetising inductance used in initial charging circuit (Stephens 2016)

The capacitances either side of the harvester (ground and conductor) were measured by removing the one and inserting the multimeter in its place and considering the system as a general impedance voltage divider (Figure 3.14). This was performed to understand the divider's capacitance ratio more than the absolute values themselves as this method is prone to inaccuracies brought about by the multimeter leads themselves likely to contribute to stray capacitances. These figures were nonetheless simulated to aid in verifying (or otherwise) experimental data. Capacitances measured were:

- Conductor to Harvester Capacitance - 24.41pF (130.4 MOhm @ 50Hz)
- Harvester to Ground Capacitance – 127.5pF (25.0 MOhm @ 50Hz)

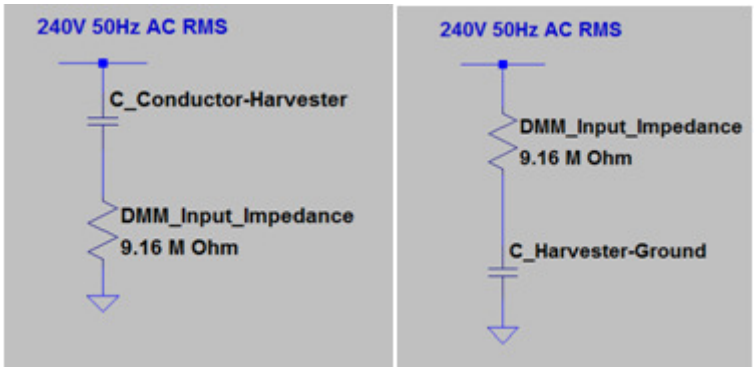

Figure 3.14 – Equivalent test circuits to determine system capacitances present (Stephens 2016)

The values obtained were much larger than expected using the formulas utilised by Zhao et al (2012) and will be discussed in chapter 6. It is worth noting however that estimates obtained by Zangl et al (2009) were also significantly larger than that of Zhao for similar scenarios thus pointing to a possible area that is not adequately addressed as yet.

The measured capacitance values were inserted into the LTSpice simulation for the harvester circuit including the transformer as shown in Figure 3.15. The output waveform shown is the charging voltage of the storage capacitor. The maximum reached here is approximately 800mV which is not at all expected. The maximum voltage reached is expected to be set by the secondary voltage, which is in turn set by the voltage across the top half of the voltage divider (transformer primary voltage) as shown below.

$$V_{primary(peak)} = \sqrt{2}\, x\, 240\, x \left(\frac{130.4}{130.4 + 25}\right) = 284.8V \tag{3.4}$$

$$= V_{primary(peak)} x \left(\frac{\sqrt{998.8}}{\sqrt{44.1}}\right)$$

$$V_{\mathrm{sec}(peak)} = 59.84V = V_{final\ storage}$$

Attempts to understand and rectify this problem with the simulation were unsuccessful but the experiment went ahead regardless. As mentioned previously it was uncertain whether this initial test with the transformer was going to correctly harvest energy for the reasons stated.

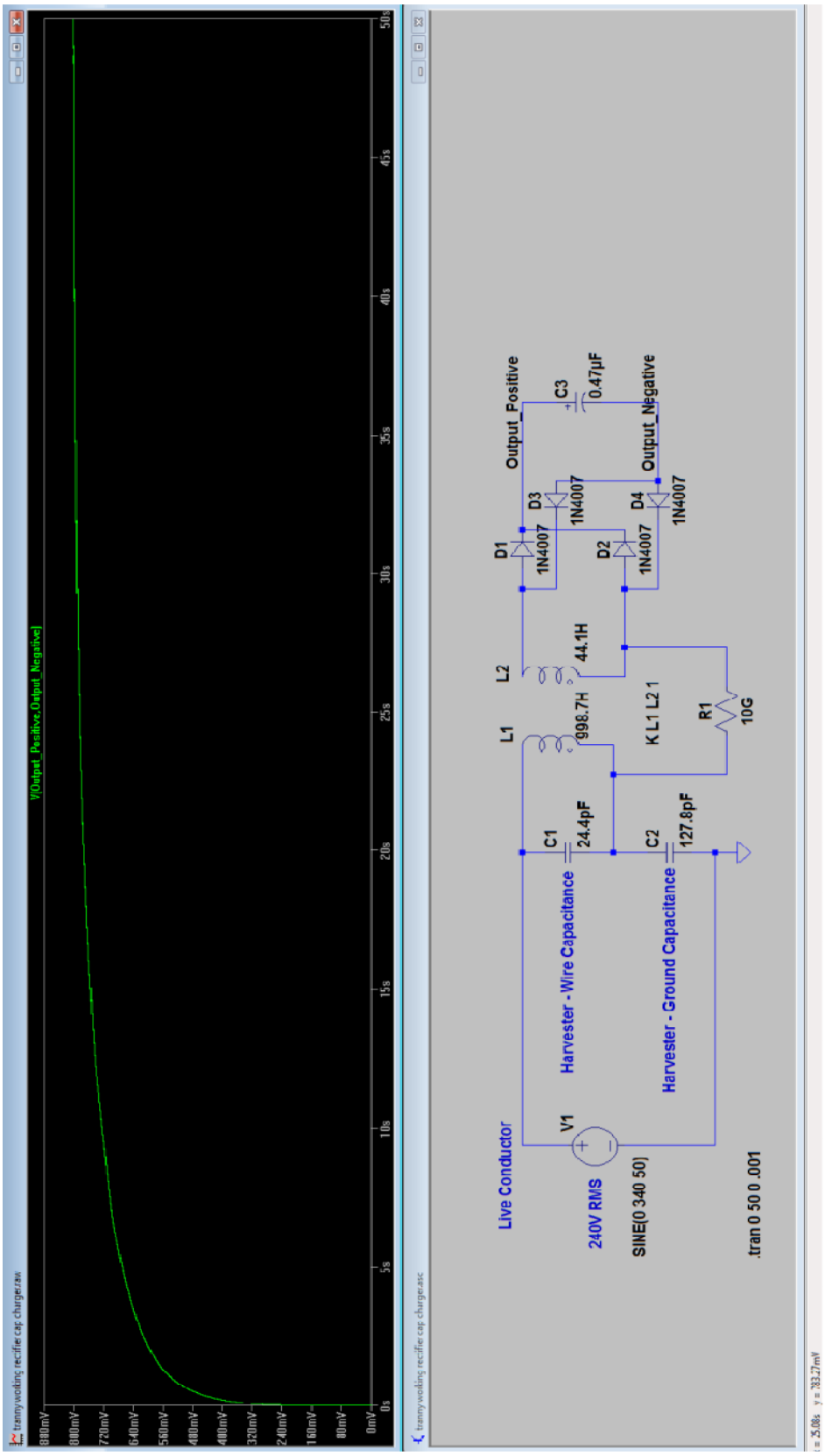

Figure 3.15 – Output from 240V harvester circuit simulation with transformer (circuit adapted from Zangl 2009)

The experiment conducted was actually successful in charging the 0.47uF storage capacitor in some scenarios. The results are tabled and discussed in Chapter 6.

The main experiment setup is described by the circuit below (Figure 3.16) along with the simulation output and expected results. The voltage reaches a maximum of approximately 280V which is close to the expected maximum voltage of 284.8V calculated from the impedance voltage divider at 50Hz. The maximum is reached in approximately 3500 secs (about 58 mins) equating to approximately 250uW average power being delivered to the 22uF storage capacitor.

The experiment was conducted and the results are detailed in Chapter 6.

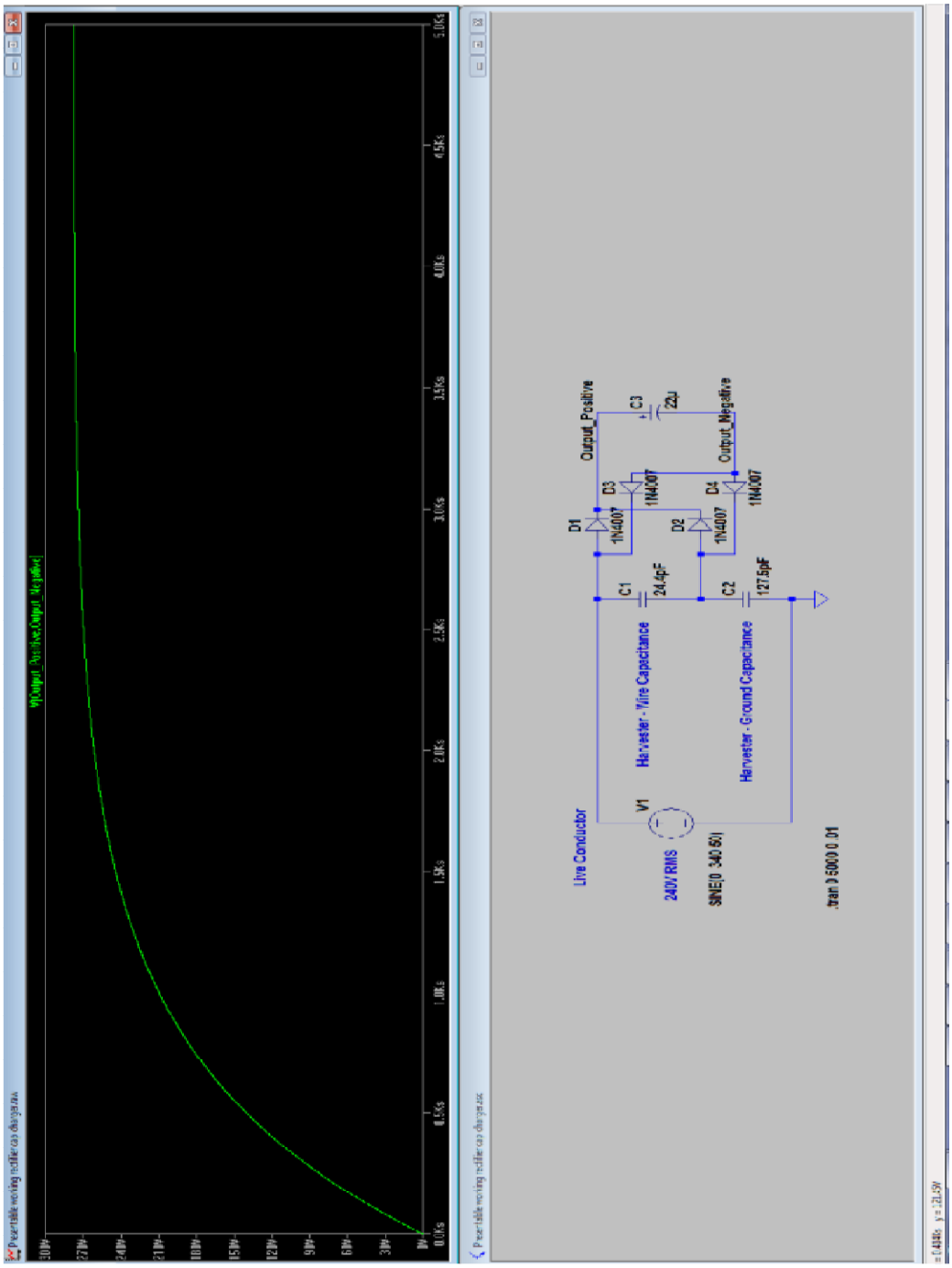

Figure 3.16 – Output from 240V harvester simulation with transformer omitted (circuit adapted from Zangl 2009)

4 Fault Detection and Mapping Development

4.1 Introduction

The fault detection function, along with its timely communication of alerts to local protection infrastructure, is the primary role of the proposed system. Any deployed system must meet minimum reliability, repeatability and accuracy standards to ensure safety and quality of service for SWER line power customers.

4.2 Fault Detection

The fault detection function, along with its timely communication of alerts to local protection infrastructure, is the primary role of the proposed system. Any deployed system must meet minimum reliability, repeatability and accuracy standards to ensure safety and quality of service for SWER line power customers.

As the system is proposed to complement the existing over-current type protection, the type of faults being monitored by this system will be of the high impedance type. Detection of this type of fault was summarised in section 2.3.2 by Kawady et al (2010) and Holland (2013) which basically differentiates between detection that relies upon real time HIF signature recognition (detecting arcing using waveform analysis, spectrum analysis or wavelet analysis) and that of a ‘open conductor’ logic based approach. The former will be looked at briefly here but it is expected the reliability of this method is questionable and also likely to be over taxing on the meagre hardware abilities of the onboard processors and memory capabilities given the limited available power. The latter approach conversely provides for a simple and logical solution which would suggest a reliable solution for wire break type faults.

The logic based system could conceivably be extended to not just monitoring the local Power line voltage, but with the addition of current monitoring transformers, the local current could be measured and compared against neighbouring devices to ensure there are no effective ‘leaks’ inadvertently discovering where fault current may be flowing.

4.2.1 Arc Detection

The fundamental attribute of a successful arc detection function is the ability to distinguish between the signatures of the many various types of 'normal' modern loads and that of a high impedance arcing fault. This is an area of research that has been ongoing for a number of decades and the consensus is largely inconclusive regarding its effectiveness. Its application has only really occurred in highly specialised circumstances where either a fault has already been detected or where the types of loads (and thus the type of current they draw) were previously known.

Studies by Djuric and Terzija (1995) that involved simulating arcing waveforms showed that during an arcing event the supplying voltage waveform starts to resemble a squarewave. From this premise it was shown that a continuous Fourier Transform could be performed on the voltage waveform to obtain its spectral components and then compared against that of a squarewave's spectral signature using a 'least error squares' technique. The investigation showed success for simulated arc waveforms in certain scenarios but did not equate to successful practical arc detection because the arcing waveforms proved to be much too complex and varied to reliably identify due various parameters including the nature of changing arc paths, different geometries and rates of cooling. This type of system found a relatively narrow application of detecting arcing on power lines that had already tripped over-current protection, and was attempting to assert whether the line was broken and arcing on the ground for instance.

The problem with arc detection was illustrated further by Kawady et al (2010) where an investigation was undertaken to compare the harmonic load profile of downed conductors to that of a series of common loads. Loads that were investigated included:

- A three phase 400/230V 3kW static load resistor,
- a three phase 400/230V 7.5kW induction motor,
- Single phase 230V 3.5kW Air conditioner

Kawady et al (2010) recognised also that an '...economic, versatile and dependable detector' required more research and better understanding of the underlying properties of arcing fault waveform signatures than was currently understood.

A more recent study by Wang et al (2014) compared Fourier transform techniques of arc detection to wavelet analysis techniques using synthesised data. The main focus was regarding arcing detection on DC photo-voltaic cells and concluded that the wavelet analysis was superior in that it required much lower sampling rates, used less memory

and slower processing than the fourier transform technique for similar results. On the whole however, the downfall of arc detection was again highlighted by Wang et al's suggestion '...arc faults in deployed systems are seemingly random and challenging to faithfully create experimentally in the laboratory, which makes the study of arc fault signature detection difficult'

Despite technological advancements regarding the processing power and speed of computer systems the techniques used so far do not seem to present an acceptable avenue for a standalone arc detection system. This case was strongly suggested by Li & Redfern (2001), who questioned the economies of extra investment in the area and also the implications for quality of supply if indeed detection systems based on this technology were deployed. He summarised ' ...There is always a compromise between the probability of tripping a healthy circuit and leaving a downed conductor live', and concluded that no techniques were found to be totally reliable.

4.2.2 Logical Open-Conductor Approach

The nature of distributed devices across the SWER network allow for inherent possibilities that extend further than those at single 'line side' monitoring localities. The detection of an 'open' or broken conductor is the most obvious of the advantages posed. Devices deriving their power electrostatically from the power line voltage are in a position to easily monitor the voltage simultaneously. Upon detection of a significant voltage drop the device need only have enough power in reserve to communicate the event occurrence, along with its coordinates, to neighbouring devices for reasonable a period of time (Figure 4.1). The system would then need to determine the status of devices further downstream of the alerted device in order to reliably label it is a fault.

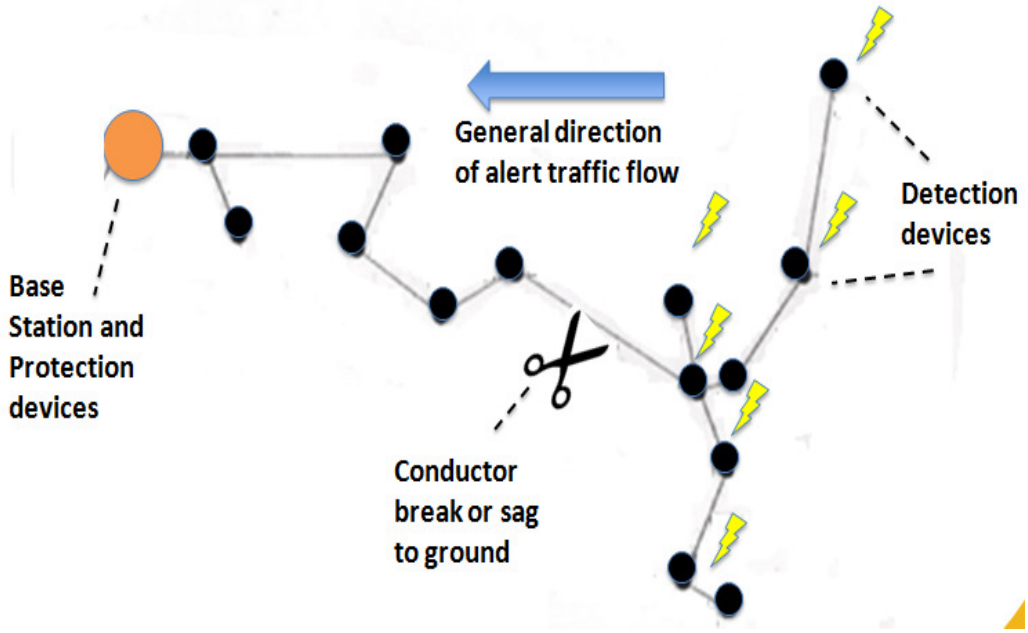

Figure 4.1 – Depiction of conductor break and response from downstream devices (Stephens 2016)

As the end goal is to prevent bushfire ignition and other obvious associated dangers with a live downed conductor, then the speed of communicating the fault to the local protection equipment becomes important. It is necessary to understand the sequence of events that must take place in order to estimate relevant quantities such as average and maximum duration times from the fault event to eventual interface with protection equipment and subsequent line trip. Accurate figures would only be obtained from running various simulations of line break faults at all locations and would be highly dependent upon the type of communications system used to convey the fault event alert.

Performance of the speed of communication would need to be judged against conventional circuit tripping theory and practice, as well as more specific bushfire related data such as that being produced by reports such as the 'Probability of Bushfire Ignition from Electric Arc Faults' by Coldham et al (2011). The Interim Report produced in 2011, studied the bushfire ignition likelihood over a range various scenarios with much attention paid to fault currents in the range of 50 and 200 amperes but also looked at the lower end of the scale at 4.2 amperes (much more relevant to the case of SWER network HIF fault currents). It was noted within the report that under worst case conditions (45°C air temperature, < 20% humidity, vegetation moisture content ~5% and wind speed of

10kph) that a fault current of 4.2 amperes produced sustained ignition 50% of the time if left for around 155 milli-seconds. In comparison, a fault that was cleared in 40 milli-seconds or less reduced the probability to essentially zero percent.

4.2.3 Nodal Analysis Approach

In the previous section harvester/detector devices will need to be deployed at almost every suspension pole (some poles may be skipped in short lengths are encountered). If devices extra devices are deployed so that either side of customer take off points (as shown below) are monitored, then it is theoretically possible to progressively 'cross reference' local currents across the entire network. The idea is that Kirchhoff's Current Law should essentially be conserved either side of any power pole or 'node' in the system. The Customer take off point will present a point where this cannot occur (mainly because there is no-where to deploy a device) and so these points would not be covered by this scheme and so devices will need to be either side of this point to minimise the unprotected section.

By referring to Figure 4.2 below, we can see that:

- I_1 should equal I_2
- I_2 should equal $I_3 + I_5$
- I_3 should equal I_4
- I_6 should equal I_7

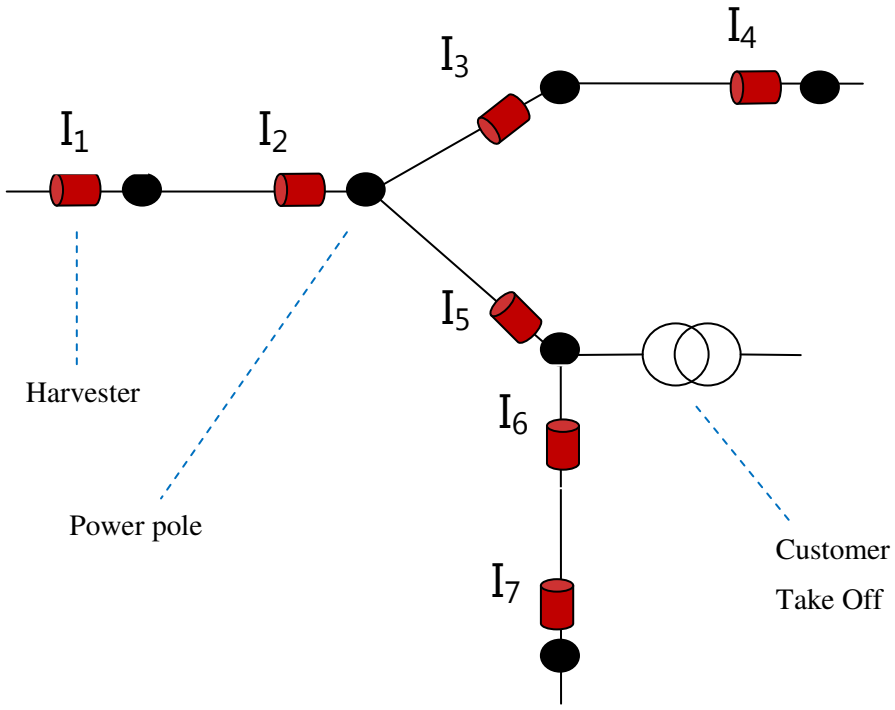

Figure 4.2 – Depiction of nodal analysis implementation (Stephens 2016)

If these equations are not conserved then there is a current 'leak' which indicates a fault (assuming measurements are accurate and within tolerances). The analysis itself will need to be undertaken in designated devices across the network and will require neighbouring devices to periodically transmit their current telemetry. Clearly this will place greater burden on the device's meagre power reserves and a trade off between the frequency of analysis (thus timeliness of any fault detection) and also power conservation. Also devices will now also need miniature current transformers and subsequent hardware componetry to measure the local current draw. Further to that a greater amount of time will need to go into manually initialising the system, as devices will need to know their relative positions within the network and which devices are to perform the analyses.

Despite these drawbacks, serious consideration ought to be given to this possibility on any actual practical deployment as it presents the opportunity to capture almost all SWER network High Impedance faults.

4.3 Mapping

The device network, and the SWER network it is distributed across, will need to be geographically defined and be locatable down to the individual device level in the event of a fault. In a line break fault situation the furthest upstream device that is reporting the fault will be inherently the closest to the fault. Service crews or the utility's administration will need to interrogate either the system via the base station gateway or the device itself to determine its location. This feature has the ability to significantly reduce the time it takes for crews to find the fault location as the fault is now narrowed down to the closest suspension pole.

To enable this functionality, devices will require low cost, low power GPS receivers such as the 'Snapshot' by Baseband Technologies that can provide occasional GPS coordinates updates to the device for it to store in memory after power cycling or re-boots. This type of technology is mature and needs no software overheads such as map or navigational systems and thus much of the cost is omitted. The hardware can in fact sit idle most of the time to save power until the device needs an update for whatever reason. Then for the devices co-ordinates can be partnered with the device's ID for any transmissions that may need to be interpreted at some stage by people.

The Base Station will however need more information than just a list of its nodes identifications and GPS co-ordinates. To aid in guarding against 'false positive' fault events it may preferable to require more than one or even several neighbouring nodes to report a line break fault (loss of voltage detection) simultaneously. Without a logical map of the nodes relative locations being known to the base station then it is not possible to recognise which nodes are neighbours to whom.

After devices are deployed across a SWER network for the first time, personnel familiar with the system would need to initialise it by creating a logical map of the devices' relative locations which will invariably follow the course of the SWER network with all its spurs and branches. This would then need to be hardcoded into non-volatile memory of the base station and the system tested until accuracy was assured.

To enact the proposed nodal analysis, information from this logical map held by the base station will need to be communicated to the relevant nodes performing the periodical nodal analysis. This could be easily achieved automatically by algorithms within the base station and nodes but does rely on the absolute accuracy of the logical map itself.

4.4 Contribution to Device Power Consumption

Ignoring any RF transmissions resulting from fault analysis and detection (this will be dealt with in the communications specification Chapter), the average powered required for the general fault detection function is analysed. Hardware that needs to support this function is:

- Sensing and peripheral circuitry
- Processing
- GPS

4.4.1 Sensing and Peripheral Circuitry

For voltage and current measurements there will require some passive (and thus power consuming) circuitry to manipulate the voltage and current signals into a usable form to provide inputs to buffers or amplifiers.

For voltage measurement it is intuitive to simply set up an extra high impedance (greater than 10Gohm total) voltage diver directly across the harvester plates (conductor and cylinder electrodes) and providing a point whereby a high impedance buffer can be connected and provide input to a ADC. The problem with this is that the cylinder electrode will not be a stable reference due to the attached charging circuit representing a ‘varying’ parallel impedance. Unless the processing code is exhaustively calibrated it will unlikely to be able to accurately determine the actual voltage present on the conductor. A significant voltage drop should still be easily distinguished from normal operation however and thus the main function of line break detection is still supported.

For the power consumption the worst case scenario for the voltage detection would occur from a 1000 volt voltage drop across a 10Gohm voltage divider which equates to 100uW.

Buffers and amplifiers for this situation will need to be carefully selected. There is generally a trade off between low power consumption and high input impedance. Two extremes are Linear Technologies’ LTC6268 which boast an input resistance of greater than 1000GOhm but also consume 16mA per amplifier. On the other side of the spectrum Maxim’s MAX9943 offer 550uA per amplifier consumption but requires up to 90nA of bias current which equates to 20Mohm input resistance. A possible trade off may be

found in Op Amps such as the LT1881 which quote supply currents of 0 .65mA per amplifier and 200pA input bias current. This would provide an input impedance of 15GOhm and approximately 2mW consumption per channel. Two channels are required and thus we can safely allocate 4mW of power to the buffer and amplifier requirements.

Current measurement (which could be omitted if nodal analysis is not required) would involve placing a brooks coil or similar within the conductors magnetic field which would be acceptable anywhere within the harvester cylinder with the caveat that it is perpendicular to the axial field lines. Using equations 2.1 and 2.3 to estimate voltage and currents for the magnetic coupling system reveals voltages of around 1- 5mV driving 5-10uA through a 700 Ohm load (calculated from 70mA flow through the conductor which is assumed to roughly be the draw from a single customer using 1kW). This will also not be difficult to drive a low power operational amplifier and power consumption concerns on this side are irrelevant as the power is drawn from the magnetic coupling of the conductor.

4.4.2 Processing

All processing will need to be performed by a dedicated ultra low power embedded microcontroller such as the 'EFM32' using the 32-Bit ARM Cortex M-3 controller. This type of MCU is expected to be required as opposed to an 'all in one' or 'System on Chip' (SoC) type modules that integrate transceivers into a monolithic type unit such as the Texas Instruments' RF430 series. These type of modules are designed for off the shelf type situations but remove some of the possibility to directly control the activity of the RF transmitter due to the tight integration of hardware and protocols.

The EFM32 will require greater design overheads than monolithic alternatives but it boasts active power consumptions around 180uA per Mega Hertz at 3V. Assuming the system was clocked at a modest 20Mhz then we can account for around 10mW consumption during active periods (which would be most of the time) plus an extra 1.3mW for two ADC's required for the sensing of voltage and current signals. A complete table of power consumption contributions is provided in the Results and Discussion Chapter.

4.4.3 GPS

Modern low cost and low power GPS receiver modules can be easily integrated into embedded systems, especially if all that is required is the occasional co-ordinate update as opposed to a suite of maps and navigational software. The main difficulty in this scenario will be in making provision for the antenna and shielding from capacitive and inductive coupling mechanisms arising from the near field radiation caused by the high voltage conductor along with the RF transmissions from the Transmitter module.

A likely candidate is Baseband Technologies' 'Snapshot' low power GPS modules that quote battery life figures of 18 days to one year from an 18mAh battery at 3V. Assuming the worst case scenario this equates to an average of 1.39mW.

4.5 Fault and Protection Systems Integration

Any fault detection system needs to be interfaced with a protection system for action to be taken on faults detected. Existing protection infrastructure on SPAusnet's Victorian SWER networks are noted to legacy type Automatic Circuit Reclosers (ACR's) with manual control only (Holland 2013), and it is expected that the remaining SWER networks operated by PowerCor have a similar situation. This presents no present opportunity to interface with the detection network proposed.

The main option involves replacing existing ACR's with remote control versions like the W- Series ACR by Schneider as shown (Figure 4.3).

Figure 4.3 – Schneider Electric W Series Remote Control ACR & associated control cabinets (Schneider Electric 2012)

Remote control sectionalisers could present a possible alternative as these could possibly compliment existing protection hardware instead of straight replacement. This would however be using the sectionaliser slightly out of scope to what it was intended considering that their use is generally to isolate circuits that have already been de-energised from an upstream recloser (Figure 4.4 shows typical deployment).

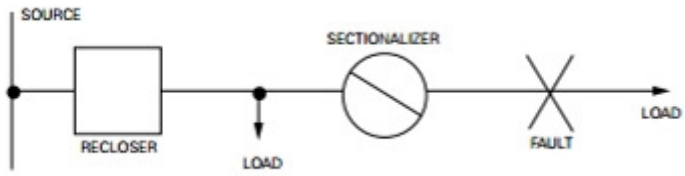

Figure 4.4 – Typical Recloser – Sectionaliser deployment (Electrical Engineering Community 2016)

The possibility that sectionalisers could open on very small fault currents such as those existing for 12.7kV SWER high impedance faults would need to be investigated.

5 Communications System Specification

5.1 Introduction

To specify a communications system for this application in terms of a conventional fixed set of specific constraints would be an unnecessary road block to a successful design and regardless would be impossible to do without almost completing the design first. With this in mind, this chapter attempts to focus on the most arduous of requirements in order to build some framework around how a design should be attempted.

5.1.1 A Word on Security

It should be noted that security concerns have not been addressed here as it has been considered out of scope. Any design must consider security issues throughout all the relevant OSI layers and likely from an overall system approach as well.

Implementing security in this type of wireless mesh network will be tough because nodes are more susceptible attacks than their wired alternatives and they have much less computational power to execute things such as encryption, decryption, certificate and key authentications etc. The key here will be to attempt to quantify ‘how much’ security is needed that adequately addresses the fact that parties could potentially ‘hack’ the system and cause the local SWER network to trip. This could well be a decision that is deferred to utility companies or political decision makers but the emphasis for the engineer must be on quantifying the risk of a compromised network, the cost of implementing different levels of security and to make an informed recommendation.

5.1.2 Presentation of Simultaneous Requirements

Table 5.1 – Presentation of Wireless Communications Simultaneous Requirements

Requirement	Specification (Quantitative)	Specification (Qualitative)	Comment
Min Range	2km (LOS)		Trade off - Isotropic radiation for meshing or directional for distance?
ISM frequency	915Mhz?		Lower is better for range vs. Tx power but limited by Antenna length; opportunity for government to use purchased bandwidth?
Min Node Density	5	Each node must be within range of 2 neighbouring nodes either side	
Data Handling		Priority 'event driven' and second priority 'store and forward'	Must have the ability to prioritise data packets
Max propagation delay for fault alert	<40mS		Max time based on probable arc ignition at 4.2A in worst case conditions
Max RF radiation	1W EIRP	Digitally modulated (3mW max for analogue or no modulation)	EIRP =Effective Isotropic Radiated Power
Quality of Service (QoS)		Must include provision for guaranteed delivery	Must satisfy reliability requirements of Utility
Max Average Power Consumption per Device	Approximately 10 mW	Receiver –always listening. Transmitter -sporadic bursts when necessary.	Ability to have direct control over the transmitter activity is essential
Topology		Self Healing 'partial' mesh. Alternative paths found upon node drop out.	'Partial' implies that nodes need not all be within range of all other nodes
Base Station	1	Master, instigates integrity checks, holds database of node statuses and network structure. Interfaces with protection system or Utility SCADA.	Bigger power supply will provide opportunity to increase sensitivity and transmit power to increase range.

5.2 Communications Specification Discussion

5.2.1 Hardware and Modulation

In section 2.2.7.1 a number of typical RF transmitter, receiver and amplifier modules were considered for their relevant sensitivity, gain, transmit power and power consumption figures. These are relatively simple digital modules and modulation techniques are generally limited to Frequency Shift Keying (FSK) and On Off Keying (OOK).

Data rates for FSK can be automatically scaled up or back according to the link's signal to noise ratio (SNR). The greater the SNR, the more discrete frequency elements can successfully be recovered to represent a greater number of symbols. Considering it from a range perspective, if extra range is required there will be an associated lower SNR. It therefore becomes more difficult to differentiate between frequency shifts and so the shifts themselves are increased making communication still possible but with a lower number of possible symbols being represented and thus a lower data rate.

On Off Keying as the name suggests is a very simple form of digital modulation technique with the simplest form basically being the presence of the carrier wave during a fixed period being a 'one' and the absence of the carrier being a 'zero'. Any binary encoding techniques can be used such as Morse code.

A design decision will be needed to be made early on between these types of hardware and modulation techniques taking into consideration expected data rates, range and power consumption. It is expected that a separate RF amplifier module is required to provide significant gain (approximately 10 -20dB) to the output of the chosen transceiver.

5.2.2 Medium Access Control

It is expected that to achieve predictable levels of reliability and Quality of Service (QoS) for a complex and dynamic situation such as a wireless mesh, synchronous type medium access control methods (TDMA) will be required. However during design other methods should be looked at such as CSMA/CA (Carrier Sense Multiple Access with Collision Avoidance) that implement 'back off' algorithms to deal with medium access contention.

This will especially be the case if synchronous methods are deemed to introduce too much delay. Considering that data rates are expected to be very low, asynchronous methods may actually be favourable to TDMA but the main issue will be the fact that for

5.2.2.1 TDMA with Spatial Re-Use

TDMA (Time Division Multiple Access) allocates time slots for nodes to transmit to guarantee against contention or conflicts. In its pure form it is synchronous and from this method provides means to accurately predict delay times per 'hop' (node to node communication'). It can introduce Quality of Service (QoS) by allocating segments within a slot to 'guaranteed delivery' and 'best effort delivery' traffic data as well as a control segment which includes such operations as synchronising and routing table updates.

For this application the ability to obtain QoS metrics such as maximum total time delays for guaranteed traffic is beneficial but its downfall has historically been that those delay times can be significantly greater than asynchronous methods if not designed carefully with little wasted bandwidth.

Spatial Re-Use (Djukic & Valaee 2007) is a method that becomes useful with partial mesh networks like the one proposed and can be simply thought of as multiple pairs of node to node communication using the same time slot because they are out of range and do not conflict with each other. Djukic presents a solution to utilise the idea of spatial re-use within a wireless mesh network which complies with IEEE801.16. The paper focuses on minimising the scheduling delay (which accumulates at every hop over the network – see Figure 5.1). It is based on determining the link bandwidths (defined by the number of slots a link can use within a frame) at the initialisation stage and then using a modified Bellman-Ford algorithm to design schedules that minimise TDMA delays. These delays generally occur when data packets requiring to be forwarded are not received in time to be transmitted in the time slot usually allocated for that particular link. Subsequently it must wait until the next opportunity occurs, with this waiting time representing the TDMA delay.

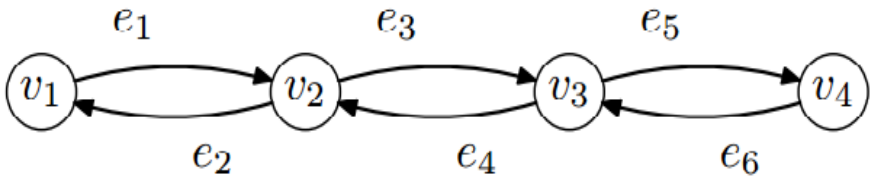

Figure 5.1 – Multiple hops between nodes causing TDMA delays (Djukic 2011) – v_i are nodes and e_i are directional links

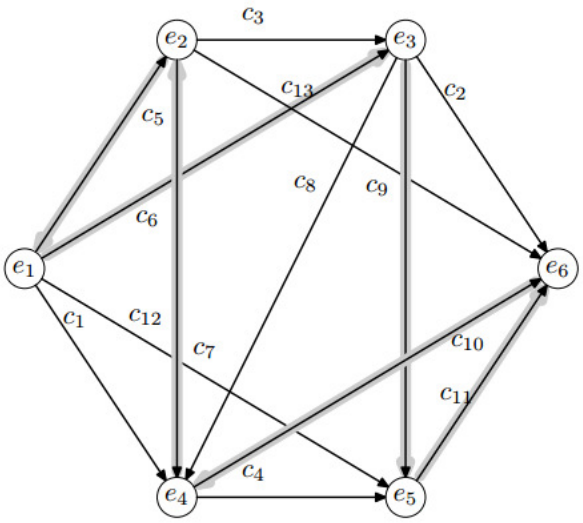

Figure 5.2 – Cluster of nodes and their respective 'conflicts graph' (Djukic 2011) – c_i are the conflicts, e_i are the nodes. Each node requires their own conflict graph to base their local scheduling and then harmonising needs to occur with neighbouring nodes

The network is initialised thus:

- Nodes establish local links (Figure 5.2)
- Nodes gather conflict information
- Nodes establish local schedules
- Nodes attempt to harmonise schedules with neighbours
- Base Station sends a 'schedule detection wave' down through the network
- The wave reaches the 'leaf' nodes and instigate waves back to the Base Station
- The nodes add information to the wave as it passes by

- The Base Station collates the information and determines if all schedules have 'converged'
- Activation of the network occurs when all schedules have converged
- A loss of a node will result in loss of convergence and thus the procedure is repeated

Djukic describes the ability to estimate the maximum TDMA delay as the time it takes for the longest return path to be travelled with the equation

$$D_{max} = \frac{2h}{H} T_f \tag{5.1}$$

Where D_{max} is the maximum delay, h is the 'height' of the tree, H is the amount of spatial re-use applied and T_f is the frame duration.

For our purposes the longest delay of particular interest is the time it takes for the furthest 'leaf' node to send an 'alert packet' or 'fault packet' to the base station. This would be half the tree height. To obtain a frame duration we would need to consider the maximum amount of slots that would be required during a frame. It is assumed that the total amount of data from all nodes contributing to their local frame allocation will easily fit into the minimum 2mS frame duration as defined by IEEE802.16.

The next step is to determine maximum a 'tree height' which is the greatest number of nodes that will be encountered from the end of a SWER network to the base station. If we take the longest SWER network to be 20km and devices place at every suspension pole with 205m average spans then we have a height of 98. This provides a maximum duration time of 196mS if no spatial reuse was enacted.

It is worth recalling here that a requirement of the system is to have fault alerts taking less than 40mS to be communicated to help ensure bushfire ignition does not occur. Clearly this system needs a spatial reuse figure of at least 5 to come close to attaining this figure that needs to incorporate an interface with protection circuit as well. Considering the network is considerably spread out with very low node densities it is expected that this figure is attainable.

5.3 Power Consumption Calculation

To obtain power consumption estimations for the communications section a fundamental or 'first principals 'type approach is used with multiple being assumptions made. Firstly an estimation of the lin budget required is found by using equation t.t and assuming that isotropic antennas are used as opposed to directional. This will be a key design element as there is a trade off here of line of sight range and the ability to mesh with adjacent nodes (on different SWER branches) for increased network reliability, but for now it will be assumed that the redundancy of the mesh is more important and thus isotropic antennas will be assumed.

Next it will be assumed that the antennas have transmit and receive gains of 0dBi and the range we are after is 2km. Using the figures from Microchip's MRF89XAM9A Transceiver module we obtain a sensitivity figure of -105dBm (which consumes a constant 6.5mW in active listening mode). We obtain the minimum transmit power according to the Friis Free Space link budget equation below

$$P_t = P_r - G_t - G_r - 20\log\left(\frac{\lambda}{4\pi}\right) + 20\log(d) \tag{5.2}$$

$$P_t = -7.33dBm = 185uW$$

However this assumes no path loss at all. Using the rule of thumb that accounts generally for path loss as discussed in the communications literature review:

- *120db link budget is needed at 433Mhz to achieve 2000m.*
- *Plus 6db doubles this distance*
- *Double the frequency - half the range*

It follows that we require a 126dB link budget which forces a transmit power of 21dBm or 126mW. Judging from the transmit powers and corresponding transmit consumption figures in Table 2.1, it is clear that the efficiency ratios of different modules lie between 0.346 and 0.179 with the stand alone amplifier being the most efficient. As our

requirements closer match the transmit power capabilities of the Texas Instruments TRF37C73 RF amplifier, thus the efficiency factor used is 0.346 which obtains an active power consumption of 364mW (burst only).

To obtain average power for the transmitter an estimation of how long and often the transmitter is active is required. Clearly this will be proportional to the quantity of and frequency of data transmission required. As fault event data is rarely encountered this can be safely ignored assuming enough energy is stored in the battery for this type of event. If periodic nodal analysis is implemented as described in section 4.3.2 then devices will constantly need to transmit their current data to neighbouring nodes. To limit the amount of time a possible fault goes undetected then it will likely be necessary to transmit once every TDMA frame (see section 5.3.2) which was assumed to be 2mS. As the sensitivity of the MRF89XAM9A of -105dBm was quoted when using a 25Kbs FSK bit rate, and assuming all information could fit within a 16 bit packets (optimistic) then we obtain an active time of 640uS. From this we obtain an average power consumption of 116.5mW which may well be prohibitive.

If nodal analysis is omitted from the fault protect6ion scheme and line break faults are solely focussed on then transmitter active times can be reduced significantly. If we can then assume that periodic transmissions can be user defined and the design of which will revolve around how often the network integrity should be checked. Assuming this is checked once a minute and is instigated by the base station in a downstream then reverse upstream wave of transmissions across the network, then nodes will need to transmit twice every minute. As data will accumulate from every node across many hops then the total amount of data per transmission will be much larger. If we assume a maximum of 200 nodes per network each contributing 16 bits of data then transmissions will need to cater for up to 3.2kbits. This equates to transmitting 128mS every minute resulting in an average power of 777uW.

Understandably much has been assumed here and the fact remains that any design that has power consumption in mind can and will need to analyse the tradeoffs between it and network integrity and other factors such as security , housekeeping and condition monitoring overheads. For simplicity and a measure of surety, a total figure for average transceiver (receiver plus transmitter) power will be set to a 10mW requirement.

6 Results and Discussion

6.1 Chapter Overview

This chapter brings together results from the 240V energy harvesting experiments along with commentary on their validity and the implications on the simulation models. Outputs from 12.7kV SWER scenario simulations are presented and discussed. Conclusions are made on the likelihood of all devices being adequately powered and finally an attempt to estimate the cost of implementing the proposed system across Victoria's SWER networks is offered.

6.2 Energy Harvesting Experiment Results

6.2.1 System Capacitance Anomalies

The expected values of capacitance for the 240V scaled experiment were calculated from the geographical construction of the harvester apparatus with the following attributes:

Cylinder Radius	- 3.75cm
Conductor Radius	- 0.5mm
Cylinder length	- 27cm
Height from Ground Plane	- 60cm
Relative Dielectric	- 1

Using equations 2.5 and 2.4 we obtain the following expected electrode to ground and wire to electrode capacitances:

$$C_{EG} = \frac{2\pi\varepsilon_0 l}{\cosh^{-1}\left(\frac{h}{r_2}\right)} = 4.335pF$$

$$C_{WE} = \frac{2\pi\varepsilon_0\varepsilon_r l}{\ln\left(\frac{r_2}{r_1}\right)} = 3.48pF$$

The values that were measured of $C_{EG} = 127.8pF$ and $C_{WE} = 24.41pF$ are clearly well out of the expected range and have no bearing on the overall ratio either. At first the problem was considered to be the fault of the measurement technique, but after initial simulations using these figures and cross referencing with initial tests, it seemed much more likely that these were in fact close to the actual capacitances present.

After further investigation, it was considered that due to the experiment needing to be conducted inside a shed due to bad weather, there may be issues with stray capacitances playing havoc on the system. As the shed was constructed from steel and iron with earthed members, there were in effect many more avenues for stray capacitances to occur such as from walls, beams etc. Moving the apparatus to different locations around the shed yielded significantly different system capacitances and thus the theory was all but proven.

This result removes any possibility of verifying the above equations in testing their usefulness for the modelling of harvesting system capacitances in the rural power line scenario.

For accurate predictions of energy harvesting output for the intended SWER line application, these estimated capacitances need to have a reasonable degree of accuracy. A ‘sanity check’ is required and can be found from industry knowledge regarding standard and accepted methods of calculating or estimating parameters such as line or ‘shunt’ capacitances and associated figures for ‘charging’ current.

It was noted by Zangl (2009) from performing a finite element analysis that the disturbance of the overall electric field due to the harvester tube is hardly noticeable away

from the immediate harvester – conductor area. We can intuitively infer from this that the 'baseline' capacitance between the harvester and ground is indeed the original line or shunt capacitance of the SWER line if the harvester were not present at all. To find this figure the method of images is used as described by the diagrams and accompanying equation below to find the per meter shunt capacitance (Figure 6.1).

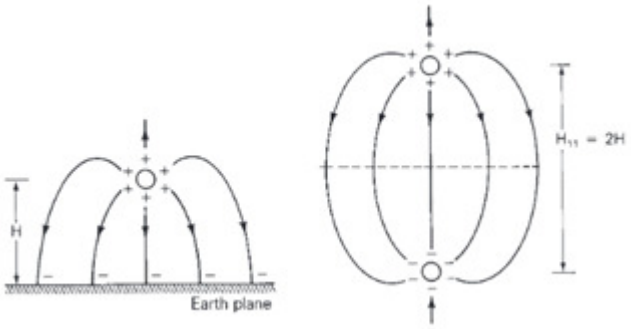

Figure 6.1 – Method of images to determine shunt capacitance for single wire system (Glover & Sarma 1994)

$$C_{shunt} = \frac{2\pi\varepsilon_0}{\ln\left(\frac{2H}{r}\right)} \quad (F/m) \tag{6.1}$$

Assuming:

- SWER Power pole height of 12.5m
- Conductor attachment height of 10.5m
- Area of interest slightly removed from power pole with height 10m
- Conductor type SCGZ with radius 0.003m

We obtain the figure of 6.32pF/m shunt capacitance which corresponds to 25.2uA per meter of 'charging' current. It is worth noting that it is generally accepted that 12.7kV

SWER has a 'charging' current of 25mA per kilometre which clearly concurs with the calculated figure (Chapman 2001).

We note that equation 6.1 obtains exactly the same figure if we considered a harvester of 1m length and the harvester radius equal to the conductor itself, and so we can safely harbour a significant degree of confidence in this equation to estimate the harvester to ground capacitance. This is important as this figure essentially governs our harvester system source impedance and thus power output performance.

6.2.2 Energy Harvester with Transformer Results

AS expected the tests conducted that included the step down transformer in circuit yielded much lower outputs than those without (shown later). Some typical results for reference and comparison purposes are shown below (Table 6.1). In some cases the digital multimeter (DMM) was connected across the storage capacitor during charging and we can see that this severely affected average power (energy over time) transferred to the capacitor. It was for this reason that the number of results were limited because to get accurate figures the charging needed to be stopped before measurement could occur – and subsequently the storage capacitor would be significant discharged during the measurement and the whole charging process would need to start again. To increase the value of the capacitor to ensure a longer RC time constant with the DMM, the system needed charging times extending into hours thus also making it difficult to get many measurement results for analysis.

For measurements of this nature an electrostatic voltmeter (which have input impedances into the Giga Ohms and may not even have to contact the device under test) would be the perfect instrument but one was unfortunately unable to be procured.

Table 6.1 – Initial experiments with step down transformer included, with & without Digital Multimeter (ZIN = 9.16Ohm)

Experiments – 0.47uF Storage Capacitor	Voltage on Storage Capacitor	Instantaneous Power dissipated into DMM	Average Storage Power
30 seconds charge time DMM in parallel with storage capacitor	14V	21uW	1.5uW
30 seconds charge time No DMM	45V	N/A	15.9uW
10 mins charge time No DMM	260V	N/A	26.5uW

6.2.3 Main 240V Experiment Results

The main experiment involved removing the step down transformer and charging a 22uF capacitor and the results are shown below in Figure 6.2, with data in Appendix F.

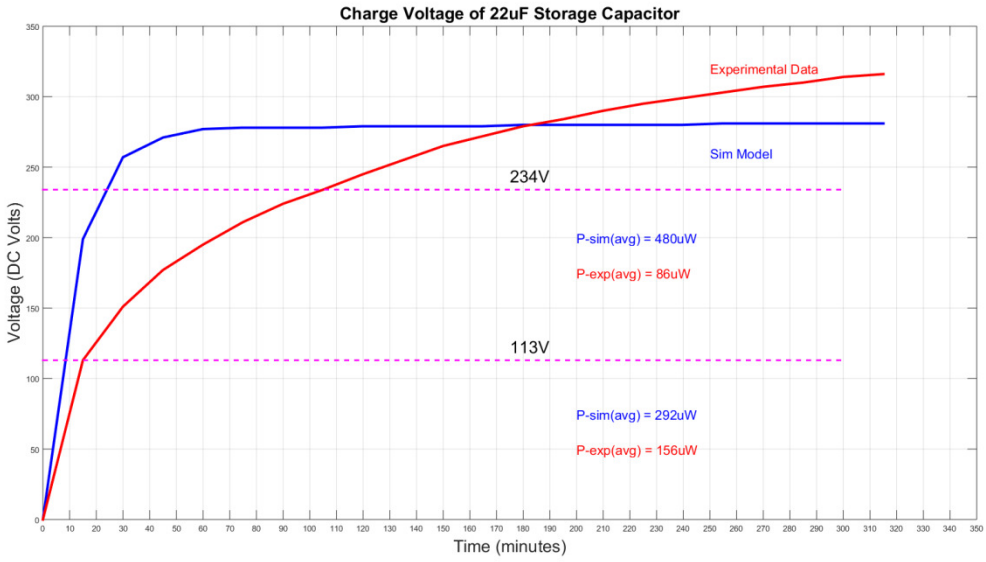

Figure 6.2 – Actual charging waveforms vs. simulated waveforms from 240V scenario experiment (Stephens 2016)

A clear discrepancy exists between the simulation model and the test results in regards to the charging rate and also the maximum charge voltage obtained.

The charging rate is believed to be significantly affected by the leakage current in the standard 450V 105°C aluminium electrolytic capacitor used to store the charge. The capacitor manufacturer in this Jamicon does not publish data on leakage current but similar capacitors from other manufacturers quote figures that are proportional to the capacitance value and the applied voltage in addition to a constant of anywhere between 1-10uA. This is very significant considering the initial source currents were expected to be in the order of 10uA RMS (see Figure 6.3 where the solid blue is showing the peak to peak source currents entering the harvester circuit).

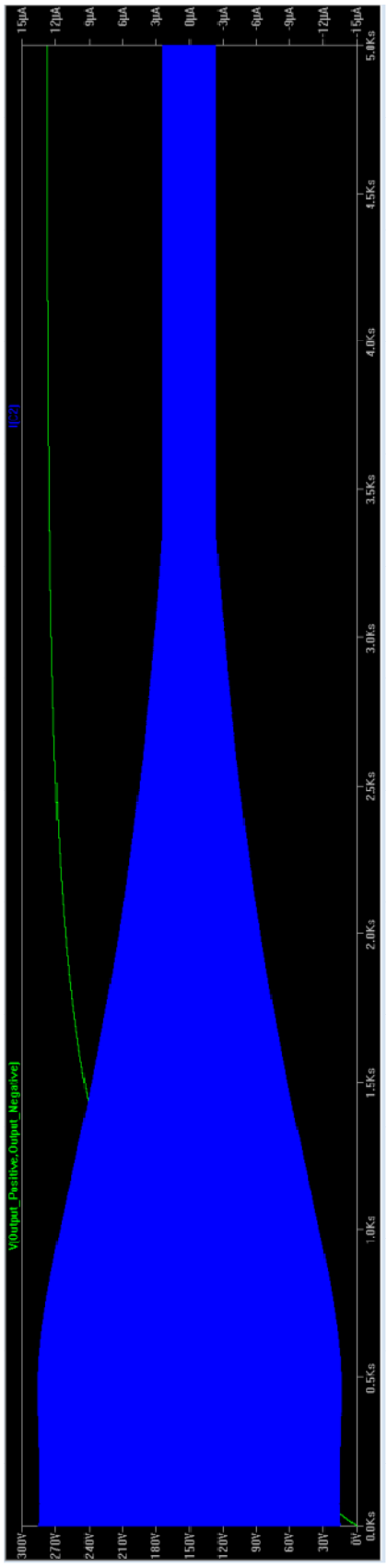
15µA
12µA
9µA
6µA
3µA
0µA
-3µA
-6µA
-9µA
-12µA
-15µA
5.0Ks
4.5Ks
4.0Ks
3.5Ks
3.0Ks
2.5Ks
2.0Ks
1.5Ks
1.0Ks
0.5Ks
0.0Ks
I(C2)
V(Output_Positive,Output_Negative)
300V
270V
240V
210V
180V
150V
120V
90V
60V
30V
0V

Figure 6.3 – Drop off of peak to peak source current feeding the harvester circuit from 240V simulation from experimental parameters (Stephens 2016)

This clearly will have had a major effect on the energy stored in the capacitor at any particular time and has rendered any meaningful examination of the model fruitless. It was initially investigated into taking in account the leakage current in the model but in this system the phenomena is highly non-linear and any attempt will be implemented with little confidence. A much more acceptable and simple next step would involve using types of capacitors with leakage currents orders of magnitude lower than that of the electrolytic such as Teflon and the other plastic capacitor types (polypropylene, polystyrene etc). This has not been conducted and would need to be done in future work.

The anomaly of the maximum charging voltage exceeding that of what was expected is considered to be the result of significant temperature decrease during the duration of the experiment. The experiment was initiated in the mid afternoon and extended just over five hours whereby the permittivity of the air is expected to have increased in the 'free space' between the harvester and virtual ground compared to the relatively insulated permittivity inside the sealed harvester. In this way it is expected that the system capacitances have changed and thus the voltage divider ratio has subsequently been altered contributing towards a greater voltage drop across harvester.

6.2.4 Model Performance Discussion

As highlighted in the previous section the performance of the model has not been able to be verified by the experiment due to significant oversights mainly in regard to the storage capacitor's leakage current. As such the prediction for the 12.7kV SWER scenario which will be based on this model will be unable to be stated with a high degree of certainty.

6.2.5 Extrapolation to 12.7kV SWER

It is recognised that the available power output from an electric field energy harvester deployed on a 12.7kV SWER line will struggle to power all functions of the proposed device. It is for this reason that it is considered unrealistic to attempt to insert a step down transformer into the harvester circuit due to the burden it will present. As a result the

voltages present will be significant, and thus the circuit must have components rated up to approximately 1kV. The required capacitive voltage divider present will attempt to push voltages well above this if left to continually charge. A practical circuit will need to incorporate voltage clamping mechanisms and likely a way to continually 'tap' off the stored energy into a battery or secondary super capacitor. With this in mind, the predicted 'clamped' output from a 12.7kV SWER power line electric field energy harvester is shown below (Figure 6.4). Two scenarios are shown along with their respective predicted power outputs. Power is once again calculated using the below equations 6.2 and 6.3, with results shown in Figure 6.5.

$$W_{stored}\ (Joules) = 0.5 x C_{storage}\ x\ V_{storage}^2 \tag{6.2}$$

$$P_{average}(Watts) = \frac{W_{Final} - W_{Initial}}{t_{Final} - t_{Initial}} \tag{6.3}$$

Scenario 1 attributes:

- SWER Power pole height of 12.5m
- Conductor attachment height of 10.5m
- Area of interest slightly removed from power pole with height 10m
- Conductor type SCGZ with radius 0.003m
- Cylinder radius 10cm
- Cylinder length 50cm
- Relative Permittivity of 1

$$C_{EG} = \frac{2\pi\varepsilon_0 l}{\cosh^{-1}\left(\frac{h}{r_2}\right)} = 5.25pF$$

$$C_{WE} = \frac{2\pi\varepsilon_0\varepsilon_r l}{\ln\left(\frac{r_2}{r_1}\right)} = 7.93pF$$

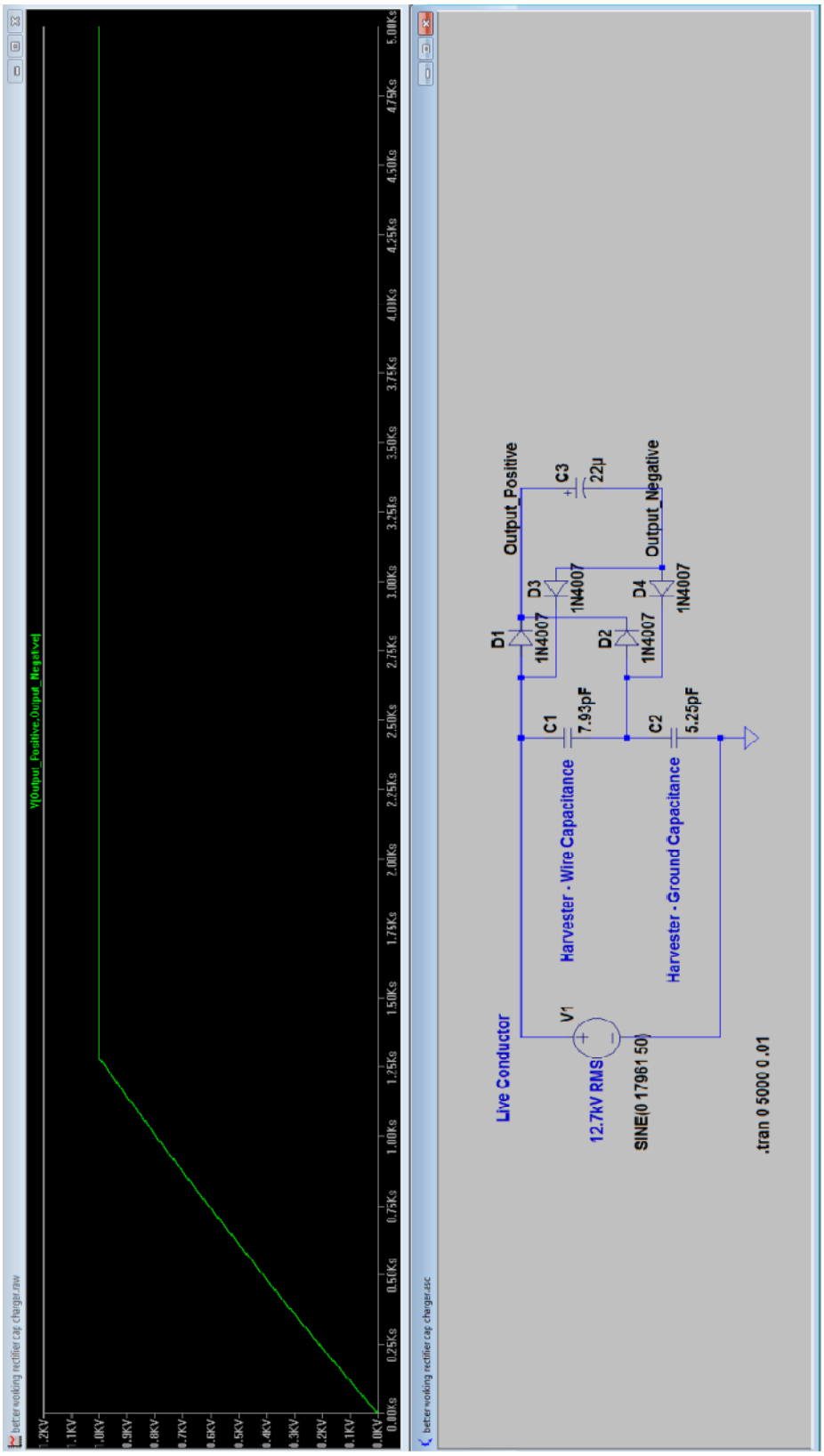

Figure 6.4 – 12.7kV SWER simulation #1 (Stephens 2016)

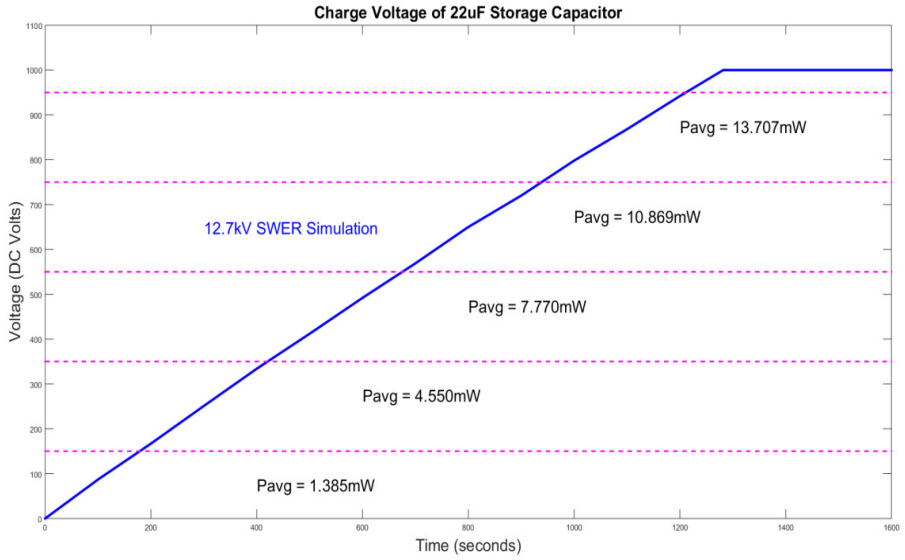

Figure 6.5 – 12.7kV SWER simulation #1 Average Power Output (Stephens 2016)

Further simulation is conducted by altering the parameters to approach practical limits to obtain maximum power outputs; results shown in Figures 6.6 and 6.7.

Scenario 2 Attributes:

- SWER Power pole height of 12.5m
- Conductor attachment height of 10.5m
- Area of interest slightly removed from power pole with height 10m
- Conductor type SCGZ with radius 0.003m
- Cylinder radius 15cm
- Cylinder length 75cm
- Relative Permittivity of 1

$$C_{EG} = \frac{2\pi\varepsilon_0 l}{\cosh^{-1}\left(\frac{h}{r_2}\right)} = 8.52pF$$

$$C_{WE} = \frac{2\pi\varepsilon_0\varepsilon_r l}{\ln\left(\frac{r_2}{r_1}\right)} = 10.67pF$$

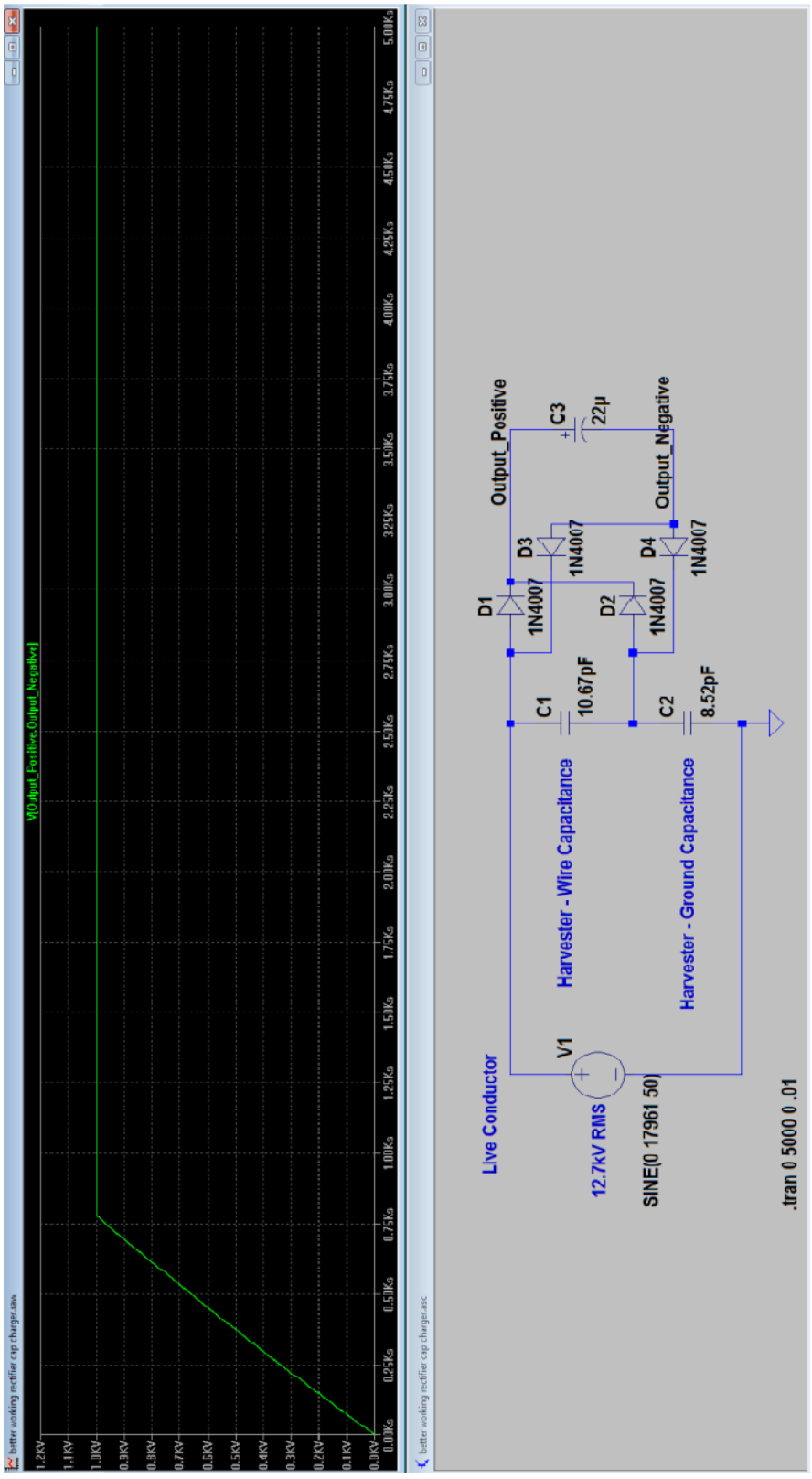

Figure 6.6 – 12.7kV SWER simulation #2 (Stephens 2016)

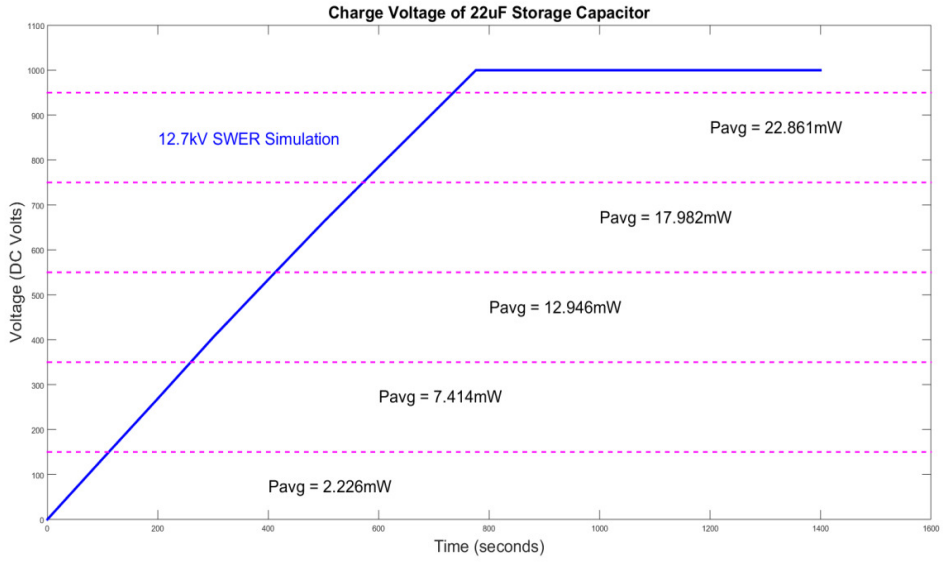

Figure 6.7 – 12.7kV SWER simulation #2 Average Power Output (Stephens 2016)

From the simulation we can see that 22.86mW is approaching a hard limit. Even this assumes deploying cylinder s of 30cm diameter and 75cm long, on rural SWER lines 10 meters in the air which will clearly be subject to all sorts of weather events. Wind resistance alone may make this size an improbability. The internal circuitry will need to overcome several problems of its own mainly in regards to the high voltages and the need for careful design work going into conditioning this power to usable voltage levels whereby a battery can be charged, without losing too much energy in the process.

6.3 Power Budget

A breakdown of the devices estimated average power consumptions are shown below in Table 6.2.

Table 6.2 – Estimated device power consumption breakdown

Device/Function	Line Break Detection Only P(avg) [mWatts]	Line Break and Nodal Analysis Detection P(avg) [mWatts]
Embedded Microcontroller Unit	10	10
Analogue to Digital Converters	0.65	1.3
Passive Circuitry	0.1	0.1
Buffers and Amplifiers	2	4
RF Transmitter Activity	3.5	116.5
RF Receiver Activity	6.5	6.5
Total	**22.75**	**138.4**

Extrapolating the simulation model to the 12.7kW SWER scenario we obtained a theoretical maximum output of 22.86mW and thus this does bring into the realms of possibly a net positive power budget (with line break detection employed only). It is however extremely tight and requires the harvester volume and shape to be awkwardly large and having the internal power supply components needing to deal with near kilovolt conditions (increasing cost and decreasing reliability).

The scenario for the nodal analysis type of detection which had the promise of capturing all previously undetected HIF faults looks to be not feasible due to the high number of local periodic RF transmissions required to keep abreast of nodal currents. The frequency could indeed be dropped and thus more average power conserved but this in turn will increase the time that possible faults go unnoticed effectively increasing the time that

protection components can trip a faulted system. In a practical deployment of the system it may be decided that to capture these extra faults, even with the delayed time to notification, might be 'better than not' employing it.

6.4 Costing Estimates

A broad picture of cost breakdown estimates for the total Victorian SWER networks is shown in Table 6.3.

Table 6.3 – Cost breakdown estimates for total Victorian SWER networks

Costs	Per Device (or per Pole)	Per Network	Total
Research and Development*	N/A	N/A	$400,000
Testing (1 Network)	N/A	N/A	$200,000
Device Hardware	$1000	$98,000	$137,200,000
Base Station	$5000	$5000	$7,000,000
Assembly	$120	$11,760	$16,464,000
Deployment	$500	$49,000	$68,000,000
Remote Control Sectionalisers or ACR's **	N/A	$50,000**	$70,000,000**
Total			**$299,264,000**
Costs	**Per Device (or per Pole)**	**Per Network**	**Total**
Maintenance and upgrades per annum (First 3 years)	N/A	$5000	$7,000,000
Maintenance and upgrades per annum (Next 10 years)	N/A	$2500	$3,500,000
Maintenance and upgrades per annum (Last 12 years)	N/A	$4000	$5,600,000
Total (Over 25 years expected lifespan)	**N/A**	**N/A**	**$123,000,000**

* Based on equivalent to 2 years work for engineers at $100 per hour.

** Assumes $50,000 per SWER network which are assumed to have an average of 20km of powerlines per circuit equating to 1400 SWER networks. Using these assumptions data was extracted from Parsons Brinkerhoff report: ESV Power line Bushfire Safety Review – Cost Benefit Analysis (2011)

The deployment of the proposed system is estimated to cost less than one tenth of the cost to replace all SWER networks across Victoria with underground cabling even when considering ongoing costs over 25 years.

7 Conclusions

7.1 Chapter Overview

This chapter is a brief look at how overall project objectives were satisfied or otherwise along with proposed future work.

7.2 Achievement of Project Objectives

- *To design a simple, reliable energy harvesting system that provides power to all device functions.*

The Energy harvesting system and its output was identified as the primary indicator of a feasible distributed device detection system. Respectively this objective was given significant attention and results show that the detection system in its simplest form (line break detection) could potentially be adequately powered. It was shown that it is unlikely more sophisticated forms of fault detection are able to be implemented due to their increased power consumption.

- *To specify a meshed communications system that can support all alarm and condition monitoring data traffic.*

It was identified that to specify a meshed communications system for the proposed network of detection devices would require significant customised approaches as off the shelf options (hardware, protocols etc) are not applicable or adequate due to the many practical constraints (reliability, timeliness, power consumption etc). Investigations

focussing on the most important elements of the system point to a design being possible but more research is required.

- *To design a logical based fault detection system that compares nodes condition monitoring data to identify faults not detectable by conventional methods.*

It was shown that an open detector logic based fault detection system should indeed be possible and implemented relatively easily. More sophisticated logic based methods were discussed such as nodal analysis to capture a greater percentage of HIFs and are promising however the extra burden on the power supply is likely to be too great.

- *To specify the system and the individual device to a level where evaluation may be undertaken.*

To properly evaluate the detection system would require a number of devices to be fully designed and deployed across a scaled system and put into fault scenarios. To model the systems with its many intractable elements such as communications, fault detection and power supply would prove to be an exercise that amounted to much greater effort than actually building a prototype system. To model individual elements such as the open conductor detection method would be an exercise in triviality and provide little insight.

7.3 Shortcomings and Possible Improvements

The greatest opportunity missed occurred during the selection of the storage capacitor for the scaled 240V energy harvesting experiment. The ‘leakage current’ parameter was not assessed and proved to a major factor in the average power produced by the harvester. Hence the experiment essentially failed to validate one way or another the models used to approximate the physical system.

7.4 Further Work

Before further work that expands on the findings of this paper, it is highly recommended that the scaled experiment be performed again with more appropriate components as mentioned in the previous section. The results of which should be used to verify models especially those involving the use of circuit simulator LTSpice.

Upon an adequate power supply being determined, a full investigation focusing on the wireless mesh communications system needs to be performed culminating in an initial design and evaluation.

Further to this a design and construction of the device including integration of power supply, processor, transceiver, sensors and casing should occur. This will inevitably be follow by prototype testing and performance analysis.

8 References

ABC 2009, 'Black Saturday death toll lowered', *ABC News (online),* 30 March 2009, viewed 22 December 2015, http://www.abc.net.au/news/2009-03-30/black-saturday-death-toll-lowered/1635324

Australian Communications and Media Authority 2008, 'Australian radiofrequency spectrum allocations chart', *(online),* Australian Government, viewed 14 April 2016, http://acma.gov.au/webwr/radcomm/frequency_planning/spectrum_plan/arsp-wc.pdf

Akyildiz, IF, Su, W, Sankarasubramaniam, Y & Cayirci, E 2002, 'A Survey on Sensor Networks', *IEEE Communications Magazine,* vol. 40, no. 8, pp. 102-114, viewed 12 May 2016, http://ieeexplore.ieee.org.ezproxy.usq.edu.au/document/1024422/?reload=true&arnumber=1024422&queryText=A%20Survey%20on%20Sensor%20Networks&newsearch=true

Akyildiz, IF & Wang, X 2005, 'A Survey on Wireless Mesh Networks', *IEEE Communications Magazine,* vol. 43, no. 9, pp. S23-S30, viewed 12 May 2016, http://ieeexplore.ieee.org.ezproxy.usq.edu.au/document/1509968/?arnumber=1509968&newsearch=true&queryText=A%20Survey%20on%20Wireless%20Mesh%20Networks

Alcaraz, C & Lopez J 2010, 'A Security Analysis for Wireless Sensor Mesh Networks in Highly Critical Systems', *IEEE Transactions on Systems, MAN, and Cybernetics – Part C: Applications and Reviews,* vol. 40, no. 4, pp. 419-428, viewed 15 May 2016, http://ieeexplore.ieee.org.ezproxy.usq.edu.au/document/5443456/?arnumber=5443456&newsearch=true&queryText=A%20Security%20Analysis%20for%20Wireless%20Sensor%20Mesh%20Networks%20in%20Highly%20Critical%20Systems

Ammar, Y, Bdiri, S & Derbel, F 2015, 'An Ultra-low Power Wake Up Receiver with Flip Flops based Address Decoder', *12th International Multi-Conference on Systems, Signals & Devices (SSD),* 16-19 March 2016, Mahdia, Tunisia, p. 1-5, viewed 10 May 2016, http://ieeexplore.ieee.org.ezproxy.usq.edu.au/document/7348127/?arnumber=7348127&queryText=An%20Ultra-low%20Power%20Wake%20Up%20Receiver%20with%20Flip%20Flops%20based%20Address%20Decoder&newsearch=true

Cantatore, E & Ouwerkerk, M 2006, 'Energy scavenging and power management in networks of autonomous microsensors', *Microelectronics Journal,* vol. 37, no. 12, pp. 1584-1590, viewed 14 October 2015, http://www.sciencedirect.com/science/article/pii/S0026269206001650

Cecilio, J & Furtado, P 2014, 'Wireless Sensors in Heterogeneous Networked Systems', *Computer Communications and Networks,* Springer International Publishing, Switzerland, viewed 16 March 2016, http://link.springer.com/book/10.1007/978-3-319-09280-5

Chapman, N 2001, 'When One Wire Is Enough', *T&D World Magazine (online),* Advance Energy, 1 April 2001, viewed 2 September 2016, http://tdworld.com/archive/when-one-wire-enough

CitiPower 2012, *Powercor prepares for bushfire season with state of the art technology*, Powercor Australia media release, Melbourne, Australia, viewed 5 November 2015, https://www.powercor.com.au/media/1179/mr-powercor-prepares-for-bushfire-season-28-nov-2012.pdf

Coldham, D, Czerwinski, A & Marxsen T 2011, 'Probability of Bushfire Ignition from Electric Arc Faults', *Report No. HLC/2010/195-B Prepared for Energy Safe Victoria,* HRL Engineering and Materials, Mulgrave, VIC, viewed 12 May 2016, http://www.esv.vic.gov.au/Portals/0/About%20ESV/Files/RoyalCommission/HRL%20-%20Interim%20report%20-%20July%202011Compressed.pdf

Djukic, P & Valaee, S 2007, 'Link Scheduling for Minimum Delay in Spatial Re-Use TDMA',IEEE INFOCOM 2007 – 26th IEEE International Conference on Computer Communications, 6-12 May 2007, viewed 27August 2016, http://ieeexplore.ieee.org.ezproxy.usq.edu.au/document/4215594/

Djuric, MB & Terzija, VV 1995, 'A New Approach to the Arcing Faults Detection for Fast Autoreclosure in Transmission Systems', *IEEE Transactions on Power Delivery*, vol. 10, no. 4, pp. 1793-1798, viewed 6 November 2014, http://ieeexplore.ieee.org/document/473378/?tp=&arnumber=473378&url=http:%2F%2Fieeexplore.ieee.org%2Fiel3%2F61%2F9986%2F00473378

Electrical Engineering Community 2016, 'How to select a sectionalizer', *Electrical installation & energy efficiency (online),* 12 February 2016, viewed 12 September 2016, http://engineering.electrical-equipment.org/safety/how-to-select-a-sectionalizer.html

Gay, D, Thompson, A, Amanulla, MTO & Wolfs, P 2009, 'Monitoring of Single Wire Earth Return systems using Power Line Communication', *Australasian Universities Power Engineering Conference (AUPEC 2009),* 27-30 September 2009, Adelaide, Australia, viewed 30 October 2015, http://ieeexplore.ieee.org/document/5357140/?arnumber=5357140

Glover, JD & Sarma, M 1994, *Power System Analysis and Design*, 2nd edn, PWS Publishing Comany, Boston

Grini, D 2006, 'RF Basics, RF for Non-RF Engineers', *MSP430 Advanced Technical Conference 2006,* Texas Instruments, viewed 9 May 2016, http://www.deyisupport.com/cfs-file.ashx/__key/communityserver-discussions-components-files/45/7585.RF_5F00_BASIC_5F00_slap127.pdf

Han, J, Hu, J, Yang, Y, Wang, Z, Wang, SX & H, J 2015, 'A Nonintrusive Power Supply Design for Self-Powered Sensor Networks in the Smart Grid by Scavenging Energy From AC Power Line', *IEEE Transactions on Industrial Electronics,* vol. 62, no. 7, pp. 4398-4407, viewed 22 September 2015, http://ieeexplore.ieee.org/document/6991534/?tp=&arnumber=6991534&url=http:%2F%2Fieeexplore.ieee.org%2Fiel7%2F41%2F7109198%2F06991534.pdf%3Farnumber%3D6991534

Helwig, A, USQ 2015, 'information extracted from KMS1 Figure 5', *2009 Victorian Bushfires Royal Commission*, WIT.5100.001.001, viewed 13 September 2015

Holland, CW 2013, *Single Wire Earth Return for Remote Rural Distribution Reducing Costs and Improving Reliability,* Maunsell AECOM, New Zealand, viewed 30 October 2015, https://www.scribd.com/document/200668307/Single-Wire-Earth-Return-System-for-Remote-Rural-Distribution#scribd

Holmes, G 2011, 'Independent Expert Report on Automatic Circuit Reclosers (ACR) for Single Wire Earth Return (SWER) distribution lines', *Powerline BushFire Safety Taskforce*, viewed 14 October 2015, http://www.esv.vic.gov.au/Portals/0/About%20ESV/Files/RoyalCommission/ACR_report.pdf

Kawady, TA, Taalab, A-MI & El-Geziry M 2010, 'Impact of Load Variations on Arcing Fault Detection in LV Distribution Networks', *Managing the Change, 10th IET International Conference on Developments in Power System Protection, Manchester, England, 29 March – 1 April 2010*, viewed 14 October 2015, http://ieeexplore.ieee.org/document/5522236/?tp=&arnumber=5522236&url=http:%2F%2Fieeexplore.ieee.org%2Fxpls%2Fabs_all.jsp%3Farnumber%3D5522236

Keutel, T, Motl, T, Bdiri, S, Viehweger, C & Kanoun O 2012, 'Robust power supply for wireless sensors using the electrostatic field of parts under high voltage', *International Conference on Smart Grid Technology, Economics and Policies (SG-TEP),* Nuremberg, Germany, 3-4 December 2012, viewed 6 November 2015, http://ieeexplore.ieee.org/document/6642365/?tp=&arnumber=6642365&url=http:%2F%2Fieeexplore.ieee.org%2Fiel7%2F6624147%2F6642357%2F06642365.pdf%3Farnumber%3D6642365

Kikkert, CJ & Reid, GD 2009, 'Is Broadband over Power-lines dead?', *Electrical and Computer Engineering, James Cook University,* Townsville, Australia, viewed 20 May 2016, http://ieeexplore.ieee.org/document/5464956/?tp=&arnumber=5464956&url=http:%2F%2Fieeexplore.ieee.org%2Fxpls%2Fabs_all.jsp%3Farnumber%3D5464956

Li, L & Redfern, M.A. 2001, 'A Review of Techniques to Detect Downed Conductors in Overhead Distribution Systems', *Developments in Power System Protection, Conference Publication No. 479 7th International Conference IEE 2001,* 9-12 April 2001, pp. 169-172, viewed 13 November 2015, http://ieeexplore.ieee.org.ezproxy.usq.edu.au/document/929290/

McLarnon, B 2005, 'VHF/UHF/Microwave Radio Propagation: A Primer for Digital Experimenters', *(online)*, viewed 9 May 2016, http://www.tapr.org/tapr/html/ve3jf.dcc97/ve3jf.dcc97.html

Magno, M, Marinkovic, S, Srbinovski, B & Popovici, EM 2014, 'Wake-up radio receiver based power minimization techniques for wireless sensor networks: A review', *Microelectronics Journal,* vol. 45, issue 12, pp. 1627-1633, viewed 10 May 2016, http://www.sciencedirect.com/science/article/pii/S002626921400264X

Maxim Integrated 2012, 'Mesh Networking Extends a PLC Network to Thousands of Meters', *Application Note 5409*, Maxim Integrated Products Inc., USA, viewed 17 May 2016, https://www.maximintegrated.com/en/app-notes/index.mvp/id/5409

Mogha, R, Yang Y, Lambert, F & Divan D 2009, 'A Scoping Study of Electric and Magnetic Field Energy Harvesting for Wireless Sensor Networks in Power System Applications', *2009 IEEE Energy Conversion Congress and Exposition,* San Jose, CA, 20-24 September 2009, pp. 3550-3557, viewed 11 April 2016, http://ieeexplore.ieee.org/document/5316052/?tp=&arnumber=5316052&url=http:%2F%2Fieeexplore.ieee.org%2Fxpls%2Fabs_all.jsp%3Farnumber%3D5316052

Nous Group 2010, 'National workshop on rural electricity network options to reduce bushfire risk', *The Nous Group Workshop, June 2010,* viewed 24 April 2016, http://earthresources.vic.gov.au/energy/safety-and-emergencies/powerline-bushfire-safety-program/swer-workshop-appendix-c

Parsons Brinckerhoff Australia Pty Ltd 2009, 'Indicative costs for replacing SWER lines', *SWER Replacement Options Report*, Department of Primary Industries, viewed 4 November 2015, http://earthresources.vic.gov.au/__data/assets/pdf_file/0003/1128864/PBReport-0908-SWER.pdf

Parth, HP & Dutta, R 2011, 'A Survey of Network Design Problems and Joint Design Approaches in Wireless Mesh Networks', *IEEE Communications Surveys & Tutorials,* vol. 13, no. 3, pp. 396-428, viewed 15 May 2016, http://ieeexplore.ieee.org.ezproxy.usq.edu.au/document/5497855/?arnumber=5497855&newsearch=true&queryText=A%20Survey%20of%20Network%20Design%20Problems%20and%20Joint%20Design%20Approaches%20in%20Wireless%20Mesh%20Networks

Popovici, E, Magno, M & Marinkovic, S 2013, 'Power Management Techniques for Wireless Sensor Networks: a Review', *5th IEEE International Workshop on Advances in Sensors and Interfaces,* pp. 194-198, viewed 10 May 2016, http://ieeexplore.ieee.org.ezproxy.usq.edu.au/document/6576090/?arnumber=6576090&queryText=Power%20Management%20Techniques%20for%20Wireless%20Sensor%20Networks:%20a%20Review&newsearch=true

Roscoe, NM, Judd, MD & Fitch J 2009, 'Development of Magnetic Induction Energy Harvesting for Condition Monitoring', *Proceedings of the 44th International Universities Power Engineering Conference (UPEC),* Glasgow, Scotland, 1-4 September 2006, viewed 6 November 2015, http://ieeexplore.ieee.org/document/5429497/?tp=&arnumber=5429497&url=http:%2F%

2Fieeexplore.ieee.org%2Fiel5%2F5426314%2F5429361%2F05429497.pdf%3Farnumber%3D5429497

Royal Commission into 2009 Victorian Bushfires (RVB) 2010, 'Electricity-Caused Fire', *Volume II: Fire Preparation, Response and Recovery,* ch. 4, pp. 147-185, viewed 30 October 2015, http://www.royalcommission.vic.gov.au/Commission-Reports/Final-Report/Volume-2/Chapters/Electricity-Caused-Fire.html

Schneider Electric 2012, *MV Pole-Mounted Automatic Circuit Reclosers - W-series*, viewed 19 March 2016, <http://www2.schneider electric.com/sites/corporate/en/products-services/energy-distribution/products offer/range presentation.page?c_filepath=/templatedata/Offer_Presentation/3_Range_Datash eet/data/en/shared/energy_distribution/w_series.xml#>.

Smith, P, Furse, C & Gunther J 2005, 'Analysis of Spread Spectrum Time Domain Reflectometry for Wire Fault Location', *IEEE Sensors Journal*, vol. 5, no. 6, pp. 1469-1478, viewed 14 October 2015, http://ieeexplore.ieee.org/document/1532290/?tp=&arnumber=1532290&url=http:%2F%2Fieeexplore.ieee.org%2Fxpls%2Fabs_all.jsp%3Farnumber%3D1532290

Srbinovski, B, Magno, M, O'Flynn, B, Pakrashi, V, & Popovici, E 2015, 'Energy Aware Adaptive Sampling Algorithm for Energy Harvesting Wireless Sensor Networks', *2015 IEEE Sensors Applications Symposium,* pp. 1-6, viewed 10 May 2016, http://ieeexplore.ieee.org.ezproxy.usq.edu.au/document/7133582/?arnumber=7133582&queryText=Energy%20Aware%20Adaptive%20Sampling%20Algorithm%20for%20Energy%20Harvesting%20Wireless%20Sensor%20Networks&newsearch=true

Standards Australia 2010, 'Overhead line design – Detailed procedures', *AS/NZS 7000:2010*, viewed 10 May 2016, http://infostore.saiglobal.com/store/details.aspx?ProductID=1439262

Tashiro, K, Wakiwaka, H, Inoue, S-I & Uchiyama Y 2011, 'Energy Harvesting of Magnetic Power-Line Noise', *IEEE Transactions on Magnetics,* vol. 47, no. 10, pp. 4441-4444, viewed 27 March 2016, http://ieeexplore.ieee.org/document/6028157/?tp=&arnumber=6028157&url=http:%2F%2Fieeexplore.ieee.org%2Fxpls%2Fabs_all.jsp%3Farnumber%3D6028157

Ullah, S & Kwak, KS 2012, 'An Ultra Low-power and Traffic-adaptive Medium Access Control Protocol for Wireless Body Area Network', *Journal of Medical Systems,* vol. 36, no. 3, pp. 1021-1030, viewed 10 May 2016, http://link.springer.com/article/10.1007/s10916-010-9564-2

Wang, Z, McConnell, S, Balog, R, & Johnson, J 2014, 'Arc Fault Signal Detection – Fourier Transformation vs. Wavelet Decomposition Techniques Using Synthesized Data', *Photovoltaic Specialist Conference (PVSC) 2014 IEEE 40th,* 8-13 June 2014, viewed 5 June 2016, http://ieeexplore.ieee.org.ezproxy.usq.edu.au/document/6925625/

Willis, S 2007, 'Investigation into long-range wireless sensor networks', *PhD Thesis,* James Cook University, viewed 31 March 2016, http://researchonline.jcu.edu.au/4306/

Willis, S & Kikkert, CJ 2006, 'Design of a Long-Range Wireless Sensor Node', *2006 IEEE Asia Pacific Conference on Circuits and Systems*, 4-7 December 2006, pp. 151-154, viewed 14 May 2016, http://researchonline.jcu.edu.au/4306/

Zangl, H, Bretterklieber, T & Brasseur, G 2009, 'A Feasibility Study on Autonomous Online Condition Monitoring of High-Voltage Overhead Power Lines', *IEEE Transactions on Instrumentation and Measurement,* vol. 58, no. 5, pp. 1789-1796, viewed 28 April 2016, http://ieeexplore.ieee.org/document/4776433/?tp=&arnumber=4776433&url=http:%2F%2Fieeexplore.ieee.org%2Fxpls%2Fabs_all.jsp%3Farnumber%3D4776433

Zhao, X, Keutel, T, Baldauf, M & Kanoun, O 2012, 'Energy Harvesting for Overhead Power Line Monitoring', *9th International Multi-Conference on Systems, Signals and Devices,* Chemnitz, Germany, 20-23 March 2012, viewed 6 November 2015, http://ieeexplore.ieee.org/document/6198106/?arnumber=6198106

Appendices

Appendix A – Project Specification

University of Southern Queensland FACULTY OF

ENGINEERING AND SURVEYING

ENG4111/ENG4112 Research Project

SPECIFICATION DRAFT 1.0

FOR:	Benjamin Mark Stephens
TOPIC:	LOW COST REMOTE SENSOR TO IMPROVE DETECTION OF LINE BREAK OR EARTH FAULTS FOR VICTORIAN SWER LINES
SUPERVISORS:	Mrs Catherine Hills Mr Andreas Helwig
PROJECT AIM:	To investigate the possibility of developing a robust and low cost sensitive fault detection and communications device for the existing Victorian SWER line network.
PROGRAMME:	(Issue A, 05 April 2016-Rev5)

1. Conduct literature reviews investigating electrostatic and magnetic induction energy harvesting techniques, long range, low data, low power wireless sensor networks implementation techniques, and high impedance, line break and earth fault detection techniques for SWER lines.
2. Specify practical and technical system requirements and limitations including the minimum fault notification time of the system, an approximate maximum cost for system rollout in Victoria and critical reliability and usability standards.
3. Evaluate the limitation of existing electrical distribution protection schemes deployed on Victorian SWER lines with particular attention on undetectable faults that have the potential to cause bushfires.
4. Investigate various methods of sensing the specific high frequency transients that are signatures of arcing and also normal current flow in SWER line conductors using non-contact technologies.
5. Investigate energy harvesting techniques from 12.7Kv SWER line conductors and produce a scaled test at 240V for evaluation with the view to estimate a minimum power budget and optimal device placement.
6. Research, and define the performance and logic specifications for low cost mesh and SWER network mapping network device to run on a minimum power budget with adequate redundancy to interface with IEC61850 and/or legacy equipment.

As time permits:

7. Build and integrate the internal electronic systems and functions into two or more devices that can be 'self powered', detect faults and communicate with each other.
8. Design and simulate a fault detection algorithm to demonstrate ways in which arcing faults might be detected.

Appendix B – Quoted SWER Characteristics

Below are a number of Victorian SWER line characteristics relevant to the project, along with their sources.

The Nous Group report (2010):

Penetration of SWER technology in Victoria

Approximate Total length of SWER powerlines in Victoria = 28000km

Typical loads

‘

SWER networks typically supply 10 -50 customers over distances up to 20km

’ SWER lines generally run point-to point,

Voltage

Victorian SWER is at a 12.7kV potential

Conductor Types

‘

Highly strung galvanised steel consisting of three strands are the most common in Victoria.

Maximum Spans

Maximum spans can be up to 1000m in special cases and often more than 500m

Parsons Brinckerhoff (2009):

Conductor Type:

'4/3/2.5 ACSR/AC line for highly loaded sections and 3/2.75 SC/GZ for lesser loaded sections and tee-offs.

Isolation transformers:

25 kVA to 1125kVA'.

Distribution transformers:

5 kVA up to 25 kVA.'

Power Poles:

12.5m wooden pole.

Maximum Span Length:

Maximum span length is 380m

Average Span Length

205m

Coldham et al (2011):

Probability of Bushfire Ignition

worst case conditions for bushfire ignition - 45°C air temperature, < 20% humidity, vegetation moisture content ~5% and wind speed of 10kph) that a fault current of 4.2 amperes produced sustained ignition 50% of the time if left for around 155 milli-seconds. In comparison, a fault that was cleared in 40 milli-seconds or less reduced the probability to essentially zero percent.

Standards Australia (2010):

Current Flow

‘

Generally 8 Amperes

Holland (2013):

Power Poles:

max height = 1

P AusNet have 521 SWER ACRs None have remote control

ACRs are placed strategically along distribution feeders and at the start of each SWER system.

Appendix C – Project Phase Breakdown

To move the project forward to achieve its aims, the following methodology is proposed:

Table 3.1: Project Phase and Task Descriptions

Phase 1	**Start Up Phase**	**Status**
1A	Further Research of energy harvesting techniques - with view to select a general design solution that best caters for the proposed application (simple, long life, low maintenance, 12.7kV , low current etc)	Complete
1B	Further Research High Impedance fault detection techniques – with view to select a general design solution that best caters for the proposed application (local/short detection range, low processing power etc).	Complete
1C	Further research into low power, low data, and long range meshed communications networks for wireless and wired mediums.	Complete
1D	Refine System Performance Specification – Narrow focus, make critical decisions on technologies, functions, methods and compatibilities	Complete
1E	Resources Check	Complete
Phase 2	**Design Phase**	
2A	Complete General System interoperability – This need only be general concepts but is needed to help define such things as power budgets and fault detection ranges which are required to set specific design criteria	Complete
2B	Complete energy harvesting prototype design	Complete
2C	Complete communications system specification	Complete
2D	Complete fault detection and device mapping design	Complete
2E	Complete overall system specification/design	Commenced
Phase 3	**Build Phase**	
3A	Build Energy Harvesting Prototype and test jig	Complete
3B	Write test program for chosen fault detection technique	Complete
Phase 4	**Test/Simulate Phase**	
4A	Test Energy Harvesting device	Completed
4B	Simulate fault detection scenarios	Complete
Phase 5	**Analysis Phase**	
5A	Energy harvesting performance	Commenced
5B	Fault detection performance	Complete
5C	System Performance	Not applicable
Phase 6	**Write Up Phase**	
6A	Draft Dissertation	Complete

6B	Final Dissertation	Complete

Appendix D – Matlab Electrostatic Harvester Model

```
% Model to calculate harvested power and energy from an
electrostatic (capacitive) energy harvester
% installed on a single phase electrical distribution conductor
%
% This model provides energy

clear all;
close all;

%Global constants
e_vaccuum = 8.854e-12; % permitivity of free space

%Harvestor Atributes
length = 0.55; % meters (m)
enclosure_radius = 0.025; % meters (m)
height = 0.5; % height from ground meters (m)
e_relative = 2.4; % relative permitivity

%Conductor atributes
Vac = 240; % Powerline Volatge Volts (RMS)
frequency = 50; % Hertz
wire_radius = 0.01; % meters (m) - (for SWER SCGZ 3/2.75 use
0.003m)

%Power conditioning and load atributes
Transformer_ratio = 120; % N1/N2 for reference (N1/N2)^2 = (L1/L2)
Magnetising_Inductance = 10000; % (Henries) L1 of transformer
Load_Resistor = 1 % (Ohms) total Resistance (including ESR) in the
RC storage ciruit
Storage_Capacitance = 1 % (Farads)
Storage_Cap_Voltage = 0.23 % (Volts) Max Cap Voltage - cut-off
circuits to protect and/or harvest

%Simulation atributes
samples= 10000;
max_time = 2000 %seconds
time = [0:(max_time/samples):max_time];

% Derived atributes
omega = 2*pi*frequency; %radian frequency
Harvestor_Capacitance =
(2*pi*e_vaccuum*e_relative*length)/(log(enclosure_radius/wire_radi
us))
Harvestor_Reactance = 1/(i*omega*Harvestor_Capacitance);
Ground_Capacitance =
2*pi*e_vaccuum*length/(acosh(height/enclosure_radius))
% Ground_Capacitance = 19e-12;
Ground_Reactance = 1/(i*omega*Harvestor_Capacitance);
Magnetising_Reactance = i*omega*Magnetising_Inductance;

% Final condition calculation
```

```
% Calculating equivalent AC resistance appearing across conductor
and harvestor electrode
%  Transformer magnetising inductance  // harvestor capacitance

Zprimary =
Magnetising_Reactance*Harvestor_Reactance/(Magnetising_Reactance +
Harvestor_Reactance);

% Capacitor Charging time is related to a final condition
(secondary voltage after rectification) if the storage
% capacitor had no upper voltage limit
% Practically Final secondary voltage appearing after capacitor is
fully charged is set
% by Storage_Cap_Voltage and enforced by overvoltage cutout
circuit

Vsec_final =  sqrt(2)*( abs(( Vac*( Zprimary/(Zprimary +
Ground_Reactance) ) )/Transformer_ratio) )

% Equivalent resistance seen by storage capacitor (treating
reactances as pure resistors and ignoring rectifier diode effects)

Req = Load_Resistor + ( ( ( (abs( Zprimary ) )*( abs(
Ground_Reactance ) ) )/( ( abs( Zprimary) ) + (abs(
Ground_Reactance) ) ) )/(Transformer_ratio^2) )




% Calculating average power from energy stored in cap over time
elapsed

if Storage_Cap_Voltage > Vsec_final
    disp('Secondary Voltage will not reach Max Capacitor Voltage')
    Energy_stored = 0.5*Storage_Capacitance*(Vsec_final^2)
    disp('Joules');


    time_elapsed = -(Req*Storage_Capacitance)*log((Vsec_final-
0.98*Vsec_final)/Vsec_final)
    average_power = (Energy_stored)/time_elapsed
    disp('Watts');

else
     Energy_stored =
0.5*Storage_Capacitance*(Storage_Cap_Voltage^2)
     disp('Joules');


    time_elapsed = -(Req*Storage_Capacitance)*log((Vsec_final -
Storage_Cap_Voltage)/Vsec_final)
    average_power = (Energy_stored)/time_elapsed
    disp('Watts');

end
```

```
 Vcap = Vsec_final + ( -Vsec_final*exp(-
time./(Req*Storage_Capacitance)) );
    for i = 1:samples
        if Vcap(i) > Storage_Cap_Voltage;
            Vcap(i) = Storage_Cap_Voltage;
        end
    end

plot(time,Vcap);
title([num2str(Storage_Capacitance),' Farad Storage Capacitor
Voltage' ,]);
xlabel('Time (seconds)');
ylabel('Capacitor Voltage (V)');
```

Appendix E – Simulation Input Parameters and Output Figures

Zangle Parameters

```
%Global constants
e_vaccuum = 8.854e-12; % permitivity of free space

%Harvestor Atributes
length = 0.55; % meters (m)
enclosure_radius = 0.15; % meters (m)
height = 4.5; % height from ground meters (m)
e_relative = 1; % relative permitivity

%Conductor atributes
Vac = 150000; % Powerline Volatge Volts (RMS)
frequency = 50; % Hertz
wire_radius = 0.03; % meters (m) - (for SWER SCGZ 3/2.75 use 0.003m)

%Power conditioning and load atributes
Transformer_ratio = 100; % N1/N2 for reference (N1/N2)^2 = (L1/L2)
Magnetising_Inductance = 3500; % (Henries) L1 of transformer
Load_Resistor = 1 % (Ohms) total Resistance (including ESR) in the RC storage ciruit
Storage_Capacitance = 4.7e-6 % (Farads)
Storage_Cap_Voltage = 50 % (Volts) Max Cap Voltage - cut-off circuits to protect and/or
harvest

%Simulation atributes
samples= 10000;
max_time = 0.005 % seconds
time = [0:(max_time/samples):max_time];
```

Zangle Simulation 1

```
>> overall_model

Load_Resistor =1

Storage_Capacitance =4.7000e-06

Storage_Cap_Voltage =50

max_time =0.0050
```

Harvestor_Capacitance =1.9011e-11

Vsec_final =14.1164

Req = 110.9557

Secondary Voltage will not reach Max Capacitor Voltage

Energy_stored = 4.6829e-04Joules

time_elapsed = 0.0020

average_power = 0.2295Watts

Zangle Simulation 2

Zangle Second Sim

overall_model

Load_Resistor = 1

Storage_Capacitance = 4.7000e-06

Storage_Cap_Voltage = 8

max_time = 0.0050

Harvestor_Capacitance =1.9011e-11

Vsec_final =14.1164

Req =110.9557

Energy_stored =1.5040e-04Joules

time_elapsed =4.3616e-04

average_power = 0.3448Watts

Zhao Parameters

```
%Global constants
e_vaccuum = 8.854e-12; % permitivity of free space

%Harvestor Atributes
length = 0.2; % meters (m)
enclosure_radius = 0.05; % meters (m)
height = 0.9; % height from ground meters (m)
e_relative = 1; % relative permitivity

%Conductor atributes
Vac = 60000; % Powerline Volatge Volts (RMS)
frequency = 50; % Hertz
wire_radius = 0.01; % meters (m) - (for SWER SCGZ 3/2.75 use 0.003m)

%Power conditioning and load atributes
Transformer_ratio = 120; % N1/N2 for reference (N1/N2)^2 = (L1/L2)
Magnetising_Inductance = 10000; % (Henries) L1 of transformer
Load_Resistor = 1 % (Ohms) total Resistance (including ESR) in the RC storage ciruit
Storage_Capacitance = 3.6 % (Farads)
Storage_Cap_Voltage = 5 % (Volts) Max Cap Voltage - cut-off circuits to protect

%Simulation atributes
samples= 10000;
max_time = 3000 %seconds
time = [0:(max_time/samples):max_time];
```

Zhao Simulation 1

```
>> overall_model

Load_Resistor = 1

Storage_Capacitance =3.6000

Storage_Cap_Voltage =5

max_time =3000

Harvestor_Capacitance =6.9131e-12

Ground_Capacitance =3.1055e-12

Vsec_final =4.8913
```

Req = 219.1662

Secondary Voltage will not reach Max Capacitor Voltage

Energy_stored =43.0652Joules

time_elapsed =3.0866e+03

average_power =0.0140 Watts

Zhao Simulation 2

overall_model

Load_Resistor = 1

Storage_Capacitance =3.6000

Storage_Cap_Voltage = 3

max_time = 3000

Harvestor_Capacitance =6.9131e-12

Ground_Capacitance =3.1055e-12

Vsec_final =4.8913

Req =219.1662

Energy_stored =16.2000 Joules

time_elapsed =749.6931

average_power = 0.0216 Watts

12.7kV SWER Parameters

```
%Global constants
e_vaccuum = 8.854e-12; % permitivity of free space

%Harvestor Atributes
length = 0.55; % meters (m)
enclosure_radius = 0.025; % meters (m)
height = 7; % height from ground meters (m)
e_relative = 1; % relative permitivity

%Conductor atributes
Vac = 12700; % Powerline Volatge Volts (RMS)
frequency = 50; % Hertz
wire_radius = 0.003; % meters (m) - (for SWER SCGZ 3/2.75 use 0.003m)

%Power conditioning and load atributes
Transformer_ratio = 120; % N1/N2 for reference (N1/N2)^2 = (L1/L2)
Magnetising_Inductance = 10000; % (Henries) L1 of transformer
Load_Resistor = 1 % (Ohms) total Resistance (including ESR) in the RC storage ciruit
Storage_Capacitance = 1 % (Farads)
Storage_Cap_Voltage = 2.7 % (Volts) Max Cap Voltage - cut-off circuits to protect
and/or harvest

%Simulation atributes
samples= 10000;
max_time = 2000 %seconds
time = [0:(max_time/samples):max_time];
```

12.7kV SWER Simulation 1

```
> overall_model

Load_Resistor = 1

Storage_Capacitance =1

Storage_Cap_Voltage =2.7000

max_time = 2000

Harvestor_Capacitance = 1.4431e-11

Ground_Capacitance =4.8353e-12

Vsec_final =2.1942
```

Req =219.1662

Secondary Voltage will not reach Max Capacitor Voltage

Energy_stored = 2.4073Joules

time_elapsed =857.3830

average_power = 0.0028Watts

12.7kV SWER Simulation 2

> overall_model

Load_Resistor =1

Storage_Capacitance =1

Storage_Cap_Voltage =1.8000

max_time =2000

Harvestor_Capacitance =1.4431e-11

Ground_Capacitance =4.8353e-12

Vsec_final =2.1942

Req =219.1662

Energy_stored =1.6200Joules

time_elapsed =376.2367

average_power =0.0043 Watts

12.7kV SWER Simulation 3

Relative dialectric = 2.4 (polystyrene)

>> overall_model

Load_Resistor = 1

Storage_Capacitance = 1

Storage_Cap_Voltage = 1.8000

max_time = 200

Harvestor_Capacitance = 3.4634e-11

Ground_Capacitance = 4.8353e-12

Vsec_final = 5.4915

Req =219.1662

Energy_stored = 1.6200Joules

time_elapsed = 87.0450

average_power = 0.0186Watts

240V Mains Simulation 1

(Parameters same as previous)

Relative dialetric = 2.4 (Polystyrene)

>> overall_model

Load_Resistor = 1

Storage_Capacitance = 1

Storage_Cap_Voltage = 1.8000

max_time = 2000

Harvestor_Capacitance =3.4634e-11

Ground_Capacitance = 8.2959e-12

Vsec_final =0.1038

Req =219.1662

Secondary Voltage will not reach Max Capacitor Voltage

Energy_stored =0.0054Joules

time_elapsed = 857.3830

average_power =6.2806e-06Watts

240V Mains Simulation 2

>> overall_model

Load_Resistor =1

Storage_Capacitance =1

Storage_Cap_Voltage =0.0800

max_time = 2000

Harvestor_Capacitance =3.4634e-11

Ground_Capacitance = 8.2959e-12

Vsec_final = 0.1038

Req =219.1662

Energy_stored =0.0032Joules

time_elapsed =322.9448

average_power =9.9088e-06 Watts

240V Mains Simulation 3

Increased conductor size

>> overall_model

Load_Resistor = 1

Storage_Capacitance =1

Appendix F – 240V Experiment Output Results

Using 22uF Storage Capacitor

Time (Mins)	Time (S)	Voltage (V)	Energy (J)	Delta Energy (J)	Average Power (W)
15	900	113	0.140459	0.140459	0.000156066
30	1800	151	0.250811	0.110352	6.13067E-05
45	2700	177	0.344619	0.093808	3.47437E-05
60	3600	195	0.418275	0.073656	0.00002046
75	4500	211	0.489731	0.071456	1.58791E-05
90	5400	224	0.551936	0.062205	1.15194E-05
105	6300	234	0.602316	0.05038	7.99683E-06
120	7200	245	0.660275	0.057959	8.04986E-06
135	8100	255	0.715275	0.055	6.79012E-06
150	9000	265	0.772475	0.0572	6.35556E-06
165	9900	272	0.813824	0.041349	4.17667E-06
180	10800	279	0.856251	0.042427	3.92843E-06
195	11700	284	0.887216	0.030965	2.64658E-06
210	12600	290	0.9251	0.037884	3.00667E-06
225	13500	295	0.957275	0.032175	2.38333E-06
240	14400	299	0.983411	0.026136	0.000001815
255	15300	303	1.009899	0.026488	1.73124E-06
270	16200	307	1.036739	0.02684	1.65679E-06
285	17100	310	1.0571	0.020361	1.1907E-06
300	18000	314	1.084556	0.027456	1.52533E-06
315	18900	316	1.098416	0.01386	7.33333E-07